JACS
JOURNAL OF THE AMERICAN CHEMICAL SOCIETY

Subscriber access provided by LUNDS UNIV

Article

Red or NIR Light Operating Negative Photochromism of Binaphthyl-Bridged Imidazole Dimer

Aya Kometani, Yuki Inagaki, Katsuya Mutoh, and Jiro Abe

J. Am. Chem. Soc., **Just Accepted Manuscript** • DOI: 10.1021/jacs.0c02455 • Publication Date (Web): 08 Apr 2020

Downloaded from pubs.acs.org on April 8, 2020

Just Accepted

"Just Accepted" manuscripts have been peer-reviewed and accepted for publication. They are posted online prior to technical editing, formatting for publication and author proofing. The American Chemical Society provides "Just Accepted" as a service to the research community to expedite the dissemination of scientific material as soon as possible after acceptance. "Just Accepted" manuscripts appear in full in PDF format accompanied by an HTML abstract. "Just Accepted" manuscripts have been fully peer reviewed, but should not be considered the official version of record. They are citable by the Digital Object Identifier (DOI®). "Just Accepted" is an optional service offered to authors. Therefore, the "Just Accepted" Web site may not include all articles that will be published in the journal. After a manuscript is technically edited and formatted, it will be removed from the "Just Accepted" Web site and published as an ASAP article. Note that technical editing may introduce minor changes to the manuscript text and/or graphics which could affect content, and all legal disclaimers and ethical guidelines that apply to the journal pertain. ACS cannot be held responsible for errors or consequences arising from the use of information contained in these "Just Accepted" manuscripts.

is published by the American Chemical Society. 1155 Sixteenth Street N.W., Washington, DC 20036

Published by American Chemical Society. Copyright © American Chemical Society. However, no copyright claim is made to original U.S. Government works, or works produced by employees of any Commonwealth realm Crown government in the course of their duties.

Red or NIR Light Operating Negative Photochromism of Binaphthyl-Bridged Imidazole Dimer

Aya Kometani, Yuki Inagaki, Katsuya Mutoh, and Jiro Abe*

Department of Chemistry, Aoyama Gakuin University, 5-10-1 Fuchinobe, Chuo-ku, Sagamihara, Kanagawa 252-5258, Japan

ABSTRACT: The development of red or near infrared light (NIR) switchable photochromic molecules is required for an efficient utilization of sunlight and regulation of biological activities. While the photosensitization of photochromic molecules to red or NIR light has been achieved by two-photon absorption process, the development of a molecule itself having sensitivity to red or NIR light has been now a challenging study. Herein, we developed an efficient molecular design for realizing red or NIR light responsive negative photochromism based on binaphthyl-bridged imidazole dimers. The introduction of electron donating substituents shows the red-shift of the absorption band at visible light region because of the contribution of a charge transfer transition. Especially, the introduction of a di(4-methoxyphenyl)amino group (TPAOMe) and a perylenyl group largely shifts the absorption edge of the stable colored form to 900 nm. In addition, because the absorption bands of one of the derivatives substituted with TPAOMe cover the whole visible-light region, the colored form shows neutral gray color. Upon red (660 nm) or NIR light (790 nm) irradiation, we observed the negative photochromic reaction from the stable colored form to the metastable colorless form. Therefore, the substituted binaphthyl-bridged imidazole dimers constitute the attractive photoswitches within biological window.

INTRODUCTION

Photochoromic molecules have received much attention because of their ability to change the molecular and the electronic structures by light. Several applications of photochromic molecules have been reported in both chemical and biological research fields for switching macroscopic bending, surface polarity, electric conductivity, catalytic activity and biological functions.[1–4] In general, photochromic molecules are classified into two-types, P- and T-type. P-type photochromic molecules have two thermally stable isomers, and the isomerization between the two isomers is reversible upon photoirradiation. On the other hand, one of the isomer of T-type photochromic molecules is thermally unstable. In particular, P-type photochromic molecules are suitable to be used to photochemical control of the two functions by using the thermal stability of the two isomers in the above mentioned applications. T-type photochromic molecules with rapid thermal back reactions will be applied to photochromic lenses,[5,6] fluorescence switching,[7,8] real-time holographic materials[9,10] and be expected as a photo-trigger to induce an instantaneous stimulus (μs–ms) to systems such as retinal in rhodopsin protein.[11] In both cases, for biological applications, the photoswitching molecule is required to have a photosensitivity to red or NIR light within the first biological window (λ = 650–950 nm), while UV light is frequently used for conventional photochromic molecules. Multi-photon absorption process has been usually used for the sensitization to red or NIR light by increasing two-photon absorption cross section and the introduction of the light-antenna units.[12–18] In contrast, the development of photochromic molecule itself showing the one-photon absorption reaction upon NIR light irradiation has been a challenging subject for organic molecular chemists[19–23] although some advances for visible light activation of the reversible photoswitches have been reported.

Negative photochromic molecules showing photoisomerization from the initial stable colored form to the thermally metastable colorless form are representative visible light responsive photoswitches.[24–31] Negative photochromism has several advantages over usual photochromism: utilization of energetically low toxic visible light and deep penetration of excitation light inside of materials. In addition, the negative photochromic molecules can be essentially switched only by single-wavelength light irradiation because the conversion ratio of the negative photochromic reaction at the photostationary state (PSS) can be adjusted by controlling the intensity of the excitation light and the thermal back reaction rate of the colorless form. The binaphthyl-bridged imidazole dimer (**BN-ImD**) is a new class of negative photochromic molecules showing the efficient decoloration upon visible light irradiation even in polar solvents.[32–35] The most thermally-stable colored form photochemically generates the short-lived biradical species (lifetime = a few tens of nanosecond) by the C–N bond breaking upon visible light irradiation. The generated biradical species has two thermal relaxation pathways, one is the thermal back reaction to reproduce the initial colored form and the other is the thermal isomerization to the metastable colorless form. The colorless form thermally goes back to the initial colored form (Scheme 1).[32] Although the rates of the thermal back reaction from the colorless state to the colored state of the negative photochromic reaction have been accelerated to the millisecond or second time scales,[36,37] the strategy for tuning of the color and the photosensitivity has not been established yet. Therefore, in this study, we investigated the efficient substitutions to the binaphthyl unit and the

Scheme 1. (a) Negative Photochromic Reaction Scheme of **BN-ImD** and the Molecular Structures of the **BN-ImD** Derivatives Substituted on (b) the Binaphthyl Unit and (c) the Imidazole Unit.

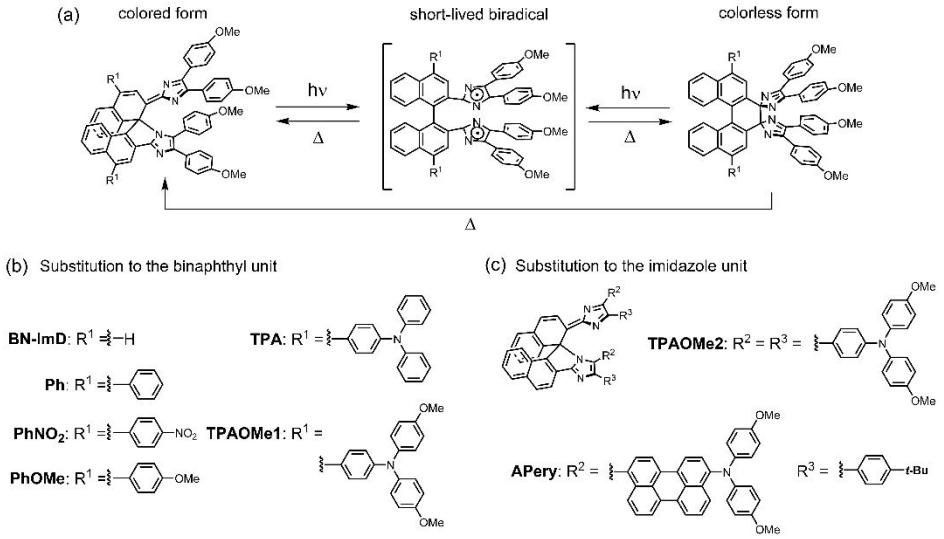

imidazole unit of BN-ImD for increasing the photosensitivity to red or NIR light.

A plausible energy consideration to presume the longest wavelength of the excitation light to induce photochromism was suggested for T-type photochromic molecules.[22] The maximum red-shift to induce the T-type photochromism can be considered to be related to the half-life of the metastable state. If the energy level of the lowest excited state is higher than the summation of the Gibbs free energy difference (ΔG^{o}) and the activation free energy ($\Delta G^{\ddagger}$) for the thermal back reaction, the ideal excitation wavelength for the T-type photochromic molecule with a half-life of seconds to minutes will be located around 1000–1200 nm. However, because this consideration assumes that the potential energy surface of the excited state is a bond-dissociation type potential, it would be difficult to presume the excitation energy for classic negative photochromic molecules such as spiropyrans having a predissociation type potential energy surface.[38–40] In contrast, this declares that the negative photochromic BN-ImD is one of the ideal molecules to develop NIR responsive photoswitches because the femtosecond spectroscopic study and the electrochemical analysis of the imidazole dimer derivatives have revealed the bond-dissociation type potential energy surface of the lowest excited singlet state.[41–44]

The characteristic absorption band at 500 nm of the initial orange-colored form of **BN-ImD** can be assigned to the ππ* transition on the diazafulvene chromophore by the TDDFT calculation.[32] This suggests that the expansion of the π-conjugation of the diazafulvene unit is efficient to induce the red-shift of the absorption band. In addition, a donor-accepter interaction becomes an efficient strategy for increasing the sensitivity to the long-wavelength light. Therefore, we introduced different types of aryl groups with electron-donating or -withdrawing natures to the 4,4'-positions of the binaphthyl unit which conjugate with the diazafulvene chromophore in the colored form in order to investigate the substituent effect, *i.e.,* the **BN-ImD** derivatives (Scheme 1b) substituted with phenyl groups (**Ph**), nitrophenyl groups (**$PhNO_2$**), methoxyphenyl groups (**PhOMe**), triphenylamino groups (**TPA**) or di(4-methoxyphenyl)amino phenyl groups (**TPAOMe1**). In addition, we also developed the BN-ImD derivatives substituted with electron-donating groups to the imidazole unit (Scheme 1c), the derivatives substituted to the imidazole unit with di(4-methoxyphenyl)amino phenyl groups (**TPAOMe2**) or di(4-methoxyphenyl)amino perylene group (**APery**).

RESULTS AND DISCUSSION

Substitution Effect on the Bridging Binaphthyl Unit

Figure 1a shows the absorption spectra of **BN-ImD**, **Ph**, **$PhNO_2$** and **PhOMe** in benzene at 298 K. The maximum wavelength of the absorption band shows *ca.* 20-nm shift to the longer wavelength by the introduction of the aryl groups. The TDDFT calculation for **Ph** clearly shows the π-conjugation of the diazafulvene unit extends to the substituted phenyl ring (Figure S83). Moreover, it was suggested that the introduction of electron-donating groups is more efficient to induce the red-shift of the absorption band than that of electron-withdrawing groups because the absorption band of **PhOMe** is slightly red-shifted, compared with that of **$PhNO_2$**. The absorption spectra of **PhOMe**, **TPA** and **TPAOMe1** in benzene are shown in Figure 1b. The introduction of TPA and TPAOMe groups makes two absorption bands in the visible and NIR light region and the absorption tail of **TPAOMe1** reached to 750 nm in benzene. It is noteworthy that **TPAOMe1** absorbs the whole visible-light region, resulting in the neutral gray color in the colored form. The changes in the absorption spectra accompanied with the negative photochromic reactions of the derivatives are shown in Figures 2 and S54. The absorption bands at 545 nm and 577 nm of **TPA** and **TPAOMe1**, respectively, can be characterized by the TDDFT calculations (MPW1PW91/6-

31+G(d,p)//MPW1PW91/6-31G(d) level of the theory). The calculations revealed that the charge transfer (CT) transition characters from the TPA or TPAOMe groups to the diazafulvene unit (HOMO–2 → LUMO transition, Figures S84 and S85) mainly contribute to the absorption bands, indicating that the diazafulvene unit possesses an electron-withdrawing nature. The absorption bands at 490 and 577 nm of **TPAOMe1** efficiently disappeared upon 642 nm laser irradiation, and the color of the solution changes from the gray to pale yellow by the negative photochromic reaction at the PSS (Figure 2). To the best of our knowledge, this is the first report of the negative photochromic reaction from a neutral gray color to colorless only by a single photochromic molecule although some examples of the conventional positive photochromic molecules showing a gray color have been reported.[45–47] This negative photochromic reaction can be repeated several times upon visible light irradiation (Figure S57).

The maximum wavelengths of the stable colored forms and the half-lives of the colorless forms in benzene at 298 K are summarized in Table 1. The time profiles of the thermal recovery processes follow the first-order reaction kinetics (Figure 3). The thermal back reaction of the colorless form decelerated by the electron-withdrawing nitro-phenyl group. On the other hand, the introduction of the electron-donating groups accelerated the thermal back reaction. The activation energies of the thermal back reactions were estimated from the Eyring plots and summarized in Table S2.

Table 1 The Maximum Wavelength of the Colored Form and the Half-life of the Colorless Form at 298 K.

	λ_{max} (nm)	$\tau_{1/2}$ (min)
BN-ImD	490	2.4
Ph	507	1.5
PhNO$_2$	513	4.5
PhOMe	516	1.3
TPA	545	1.4
TPAOMe1	577	1.2
TPAOMe2	575	0.25
APery	646	2.7

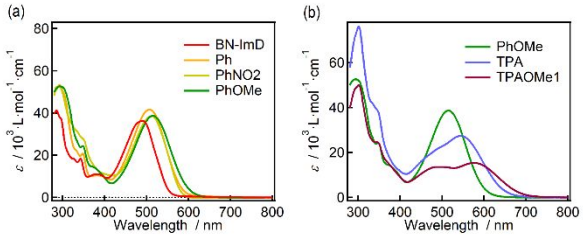

Figure 1. The absorption spectra of **BN-ImD**, **Ph**, **PhNO$_2$**, **PhOMe**, **TPA** and **TPAOMe1** in benzene.

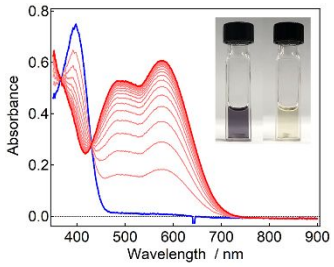

Figure 2. Thermal absorption spectral change (time interval = 60 s) of **TPAOMe1** (3.9×10^{-5} M) at 298 K in degassed benzene recorded after irradiation with red light (642 nm, 34 mW).

Since the absorption band at 577 nm of **TPAOMe1** in benzene is assigned to the CT transition, the positive solvatochromism can be expected in polar solvents. We carried out the TDDFT calculation of **TPAOMe1** including a solvent effect by the polarized continuum model (PCM–DFT, MPW1PW91/6-31+G(d,p)//MPW1PW91/6-31G(d) level of the theory). The molecular structures were fully optimized in benzene (ε = 2.247) and DMSO (ε = 46.7). The theoretically calculated absorption spectra in benzene and DMSO suggest that the absorption band characterized as the CT transition shows the red shift to the NIR light region in polar solvents (Figure S87). Figure 4 shows the absorption spectra of **TPAOMe1** in various solvents. Although the absorption band at around 500 nm assigned to the ππ* transition on the diazafulvene chromophore is not affected by the solvent polarity, the CT absorption band shifts to the longer wavelength region. In particular, the absorption edge reaches to the wavelength at 850 nm in DMSO due to the red-shift and broadening of the absorption band, and the color of the solution changes to blue. This NIR sensitivity beyond 800-nm light is comparable to the longest wavelength sensitivity of the molecule showing one-photon induced negative photochromism reported to date.[19–23] Upon NIR light (785 nm) irradiation, the absorption bands in visible light region decreases by the photoisomerization to the colorless form even in the polar solvents (Figure S55). The thermal back reaction rates also depend on the solvent polarity (Figure S79).

Substitution Effect on the Imidazole Unit

The spectroscopic investigations of the **BN-ImD** derivatives revealed the introduction of the electron-

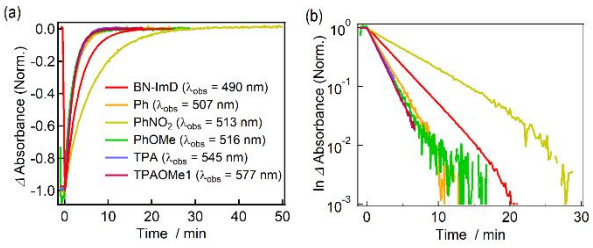

Figure 3. (a) The time profiles of the transient absorbance and (b) the logarithm plots of the time profiles of the BN-ImD derivatives in degassed benzene at 298 K.

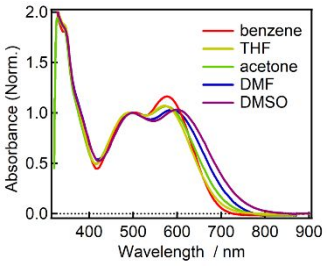

Figure 4. The solvatochromic effect of the absorption spectra of **TPAOMe1** in various solvents.

ACS Paragon Plus Environment

donating group was efficient to induce the CT transition, leading to enhance the photosensitivity to red or NIR light. Therefore, the **BN-ImD** derivatives having the strong electron donor in the imidazole unit were also developed and the photochromic properties were investigated in detail.

Figure 5 shows the UV–Vis–NIR absorption spectra of the colored forms of **BN-ImD**, **TPAOMe2** and **APery** in benzene at 298 K. The maximum wavelength of the absorption band of **TPAOMe2** shows *ca.* 85-nm shift to the red-light region, compared with that of **BN-ImD**. The absorption tail of **TPAOMe2** reached to 750 nm. While the absorption band at around 500 nm of **BN-ImD** can be assigned to the π-π* transition, the TDDFT calculation (MPW1PW91/6-31+G(d)//MPW1PW91/6-31G(d)) of **TPAOMe2** demonstrated the contribution of the CT transitions from the TPAOMe group to the diazafulvene unit (HOMO–3 → LUMO transition, Figure S88). The introduction of Apery unit is more efficient to make a new absorption band assigned to the CT transition (HOMO–1 → LUMO transition, Figure S89) in the NIR light region. The absorption tail of **APery** reaches to ca. 850 nm owing to the electron-donating ability of the APery unit. The intense absorption band of **APery** at 500 nm is attributable to the ππ* transition localized on the APery unit. Therefore, these substitutions are quite effective to increase the NIR light sensitivity even in apolar solvents. This absorption tail of **APery** is slightly red-shifted to ca. 900 nm in polar solvent as shown in Figure S80.

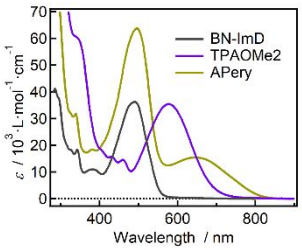

Figure 5. The absorption spectra of **BN-ImD**, **TPAOMe2** and **APery** in benzene.

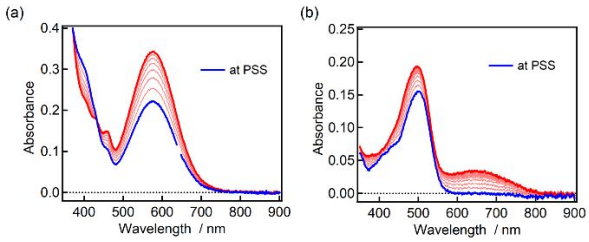

Figure 6. Thermal absorption spectral changes (time interval = 5.4 s) of (a) **TPAOMe2** (1.1×10^{-5} M) and (b) **APery** (2.9×10^{-6} M) at 298 K in degassed benzene recorded after irradiation with red light (660 nm, 270 mW)

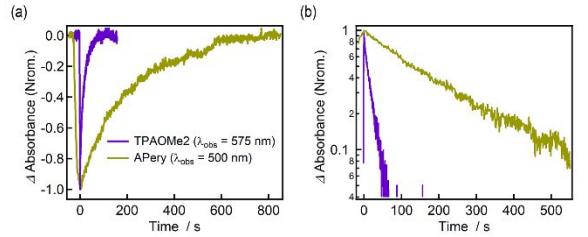

Figure 7. (a) The time profiles of the transient absorbance and (b) the logarithm plots of the time profiles of **TPAOMe2** and **APery** in degassed benzene at 298 K.

The negative photochromic behaviors of **TPAOMe2** and **APery** in benzene are shown in Figure 6a. Upon red light (660 nm) irradiation to **TPAOMe2**, the absorption band at 575 nm decreased and reached to the PSS, indicating the photoisomerization from the colored form to the colorless form. After ceasing red light irradiation, the absorption band in the visible region gradually increases. The recovery curve of the absorbance in the visible light region follows the first-order kinetics and the half-life of the colorless form is estimated to be 15 s in benzene at 298 K (Figures 7a and 7b). This thermal back reaction of **TPAOMe2** is 10 times faster than that of **BN-ImD**. This is the fastest thermal back reaction in the BN-ImD system reported to date. Therefore, the introduction of TPAOMe group to the imidazole unit is also effective to accelerate the thermal back reaction of the negative photochromism as similar to the substitution to the bridging binaphthyl unit. However, the absorption band was not completely disappeared at the PSS in this condition because of the fast thermal back reaction of the colorless form. Figure 6b shows the negative photochromic reaction of **APery**. Upon red light irradiation, the absorption band at around 700 nm completely disappeared and recovered with a half-life of 2.7 min. at 298 K. In contrast, the intense absorption band at 500 nm remained under light irradiation because this absorption band is attributable to the localized ππ* transition on the APery unit as discussed above. We also demonstrated the photoswitching of **APery** using NIR light as an excitation light source. As shown in Figure S55, the absorption band at 700 nm decreases upon 790 nm light irradiation, and therefore, this photochromism will be applicable as a NIR light responsive photo-trigger.

The conversion efficiency of the Negative Photochromic Reactions

The conversion efficiencies from the colored to the colorless forms of NIR light responsive **TPAOMe1**, **TPAOMe2** and **APery** were estimated by using 1,2-bis(2-methylbenzo[b]thiophene-3-yl)-perfluorocyclopentene (DAE) as a standard.[48] We prepared the solutions of **TPAOMe1**, **TPAOMe2**, **APery** and DAE in benzene. The absorbance of the solutions at the excitation wavelength (517 nm for **TPAOMe1** and **TPAOMe2**, 600 nm for **APery**) was matched with that of the solution of DAE. The changes in the absorbance upon laser irradiation ($\Delta OD_{colored}$ and ΔOD_{DAE}) were plotted against the laser power (see the Supporting Information) to estimate the ΔOD values per unit laser power (the slope of the plots). The conversion efficiency ($\phi_{colored}$) of **TPAOMe1** was estimated to be 0.06 from the following equation,

$$\frac{\varphi_{colored}}{\varphi_{DAE}} = \frac{\Delta OD_{colored}}{\varepsilon_{colored}} \times \frac{\varepsilon_{DAE}}{\Delta OD_{DAE}}$$

where ϕ_{DAE} (0.35) is the quantum yield of the open-ring reaction of DAE,[49] ε_{DAE} (0.91×10^4 M^{-1} cm^{-1}) and $\varepsilon_{colroed}$ of **TPAOMe1** (1.33×10^4 M^{-1} cm^{-1}) are absorption coefficients of the closed-ring form of DAE and the colored form,

respectively. This conversion efficiency is two times higher than that of **BN-ImD**. In the similar way, the conversion efficiencies of **TPAOMe2** ($\varepsilon_{colroed}$ = 2.03×10⁴ M^{-1} cm^{-1}) and **APery** (ε_{DAE} = 7.6×10³ M^{-1} cm^{-1} and $\varepsilon_{colroed}$ = 1.36×10³ M^{-1} cm^{-1}, at 600 nm) were estimated to be 0.005 and 0.002, respectively. These values are sufficient to induce the negative photochromic reactions in apolar solvent as shown in Figure 6.

The bond dissociation energy of a C–N bond has been estimated to be 300 kJ/mol corresponding to a photon energy of *ca*. 400 nm light.[50] While UV light irradiation is generally required to break a C–N bond according to the bonding energy of a C–N bond, the BN-ImD derivatives show the photochemical bond-breaking reaction upon visible or NIR light irradiation. However, this bond dissociation energy is not directly applied to the photochromic BN-ImD because the consideration of the change in the Gibbs energy (the summation of the ΔG^{o} and $\Delta G^{\ddagger}$ between the initial stable and the transient metastable state) is required to presume the bonding energy of the C–N bond.[22] Especially, by considering the stabilization of the radical generated after the homolytic bond-breaking reaction of the C–N bond by the delocalization on the diphenyl imidazole ring, the C–N bonding energy of the BN-ImD systems will be less than 300 kJ/mol. In addition, the potential energy surface of the excited state of BN-ImD is expected as the bond-dissociation type as similar with the other photochromic imidazole dimers. Therefore, the photon energy for the $S_o \rightarrow S_1$ (HOMO–LUMO) transition (calculated to be 858 nm for **TPAOMe1** and 1008 nm for **APery**, respectively) will be higher than the bonding energy of the C–N bond, leading to the NIR-light induced negative photochromic reactions. However, the smaller conversion efficiencies of **TPAOMe2** and **APery** than those of **BN-ImD** and **TPAOMe1** are due to the large contribution of the CT transition to the absorption band in the red or NIR light region. Very small changes in the absorption spectra of **TPAOMe2** and **APery** in polar solvent (Figures S81 and S82) would suggest the stabilization of the excited CT state, leading to further decrease in the conversion efficiency. It might be suggested that the potential energy surface of the S_1 state changes to the predissociation type due to the CT state. The ultrafast spectroscopy to reveal the excited state dynamics of the **BN-ImD** derivatives would be required for the future work.

CONCLUSION

We demonstrated the efficient strategy to increase the red or NIR light sensitivity of the negative photochromic **BN-ImD**. The introduction of the electron-donating groups to the bridging binaphthyl unit or the imidazole unit can make CT absorption bands in the red or NIR light region because of the electron-withdrawing ability of the diazafulvene unit. The introduction of di(methoxyphenyl)amino phenyl groups red-shifts the CT absorption band to the NIR light region and the colored form shows a neutral gray color. In addition, the substitution of di(methoxyphenyl)amino perylene groups is also effective to increase the NIR light sensitivity even in apolar solvents. These molecular designs will open up a novel application of the negative photochromic imidazole dimer as a NIR light operating photoswitch.

EXPERIMENTAL SECTION

Experimental Detail for Transient Absorption Spectroscopy. The transient absorption spectra and the time profiles of the transient absorbance were recorded on an Ocean FX multichannel detector (Ocean Optics, Inc). CUV-QPOD (Ocean Optics) equipped TC 125 temperature controller (QUANTUM) was used as a cuvette holder. The probe beam from a broadband laser driven light source, EQ-99XFC (Tokyo Instruments, Inc) was guided with a QP-600-1-SR optical fiber (Ocean Optics, Inc). Optical grade solvents were used for all measurements.

Experimental Detail for Laser Flash Photolysis Measurement to Estimate the Conversion Efficiency. The laser flash photolysis experiments were carried out with a TSP-2000 time resolved spectrophotometer (UNISOKU). The excitation pulse at 517 nm and 600 nm (pulse width, 5 ns) were provided by a Continuum Surelite II Q-Switched Nd:YAG coupled to a Continuum Panther EX OPO. The probe beam from a halogen lamp (OSRAM HLX64623) was used as the probe beam arranged in an orientation perpendicular to the exciting laser beam. The probe beam was monitored with a photomultiplier tube (Hamamatsu R2949) through a spectrometer (UNISOKU MD200) for time evolutions of the transient absorbance. The excitation intensity of one pulse was estimated by an energy detector (Gentec Electro-Optics QE12LP-S-MB) with an energy monitor (Gentec Electro-Optics MAESTRO). Optical grade solvents were used for all measurements.

Materials and Reagents. All reactions were monitored by thin-layer chromatography carried out on 0.2 mm E. Merck silica gel plates (60F-254). Column chromatography was performed on silica gel (Silica gel 60N, Kanto Chemical Co., Inc.). NMR spectra were recorded at 400 MHz on a Bruker AVANCE III 400 NanoBay. DMSO-d_6, CD_2Cl_2 and $CDCl_3$ were used as deuterated solvent. ESI–TOF–MS spectra were recorded on a Bruker micrOTOF II-AGA1. Unless otherwise noted, all reagents and reaction solvents were purchased-from Tokyo Chemical Industry Co., Ltd., Wako Pure Chemical Industries, Ltd., Sigma-Aldrich Inc. and Kanto Chemical Co., Inc. and were used without further purification.

Synthetic Procedure

Substitution to the bridging binaphthyl unit

Methyl-1-bromo-2-naphthoate (**1**) and *dimethyl [1,1'-binaphthalene]-2,2'-dicarboxylate* (**2**) were synthesized according to the literature procedure.[51] *Dimethyl 4,4'-dibromo-[1,1'-binaphthalene]-2,2'-dicarboxylate* (**3**) was synthesized according to the literature procedure.[52] *(4,4'-Dibromo-[1,1'-binaphthalene]-2,2'-diyl)dimethanol* (**4**) and *4,4'-dibromo-[1,1'-binaphthalene]-2,2'-dicarbaldehyde* (**5**)

were synthesized according to the literature procedure (Scheme 2).[53]

2,2′-(4,4′-dibromo-[1,1′-binaphthalene]-2,2′-diyl)bis(4,5-bis(4-methoxyphenyl)-imidazole) (**6**). Compound **5** (10 mg, 0.021 mmol), *p*-anisil (18 mg, 0.060 mmol), and ammonium acetate (143 mg, 1.7 mmol) were refluxed in acetic acid (1.5 mL) for 8 h. After cooling to room temperature, the reaction mixture was neutralized with aqueous NH_3. The slurry precipitate formed by neutralization was filtered off, washed with water, and then dried. The residue was purified by silica gel column chromatography (CH_2Cl_2/AcOEt = 20/1) to afford **6** as yellow solid (13 mg, 0.0134 mmol, 63 %). ^{1}H NMR (400 MHz, DMSO-d_6) δ: 12.98 (s, 2H), 8.62 (s, 2H), 8.27 (s, 2H), 8.26 (d, J = 7.52 Hz, 2H), 7.62 (t, J = 7.52 Hz, 2H), 7.36 (t, J = 7.79 Hz, 2H), 7.19 (br, 4H), 7.14 (br, 2H), 6.89 (br, 9H), 6.67 (br, 4H), 3.73 (s, 6H), 3.68 (s, 6H); HRMS (ESI-TOF) calculated for $C_{54}H_{40}Br_2N_4O_4$ [M–H]$^-$: 967.1489, found: 967.1509.

4,4′-Diphenyl-[1,1′-binaphthalene]-2,2′-dicarbaldehyde (**5-Ph**, Scheme 3). Under N_2 atmosphere, compound **5** (43.0 mg, 0.092 mmol) and phenylboronic acid (55 mg, 0.40 mmol) were added to degassed THF (2 mL) and 1 M aqueous Na_2CO_3 (0.55 mL) and tetrakis(triphenylphosphine)palladium (0) (38 mg, 0.022 mmol) was added. The mixture was stirred at 70 °C for 16 h. After celite filtration, the filtrate was transferred to a separation funnel and extracted with AcOEt. The organic layer was collected and the aqueous phase was extracted with AcOEt. The combined organic layers were washed with water and brine, and AcOEt was evaporated in vacuo. The crude mixture was purified by silica gel column chromatography using CH_2Cl_2/hexane = 7/3 and used in the next step without further purification. ^{1}H NMR (400 MHz, $CDCl_3$) δ: 9.75 (s, 2H), 8.16 (s, 2H), 8.10 (d, *J* = 8.52 Hz, 2H), 7.66–7.64 (m, 2H), 7.64–7.62 (m, 3H), 7.62–7.60 (m, 2H), 7.60–7.59 (m, 3H), 7.58–7.57 (m, 2H), 7.55 (t, *J* = 1.6 Hz, 1H), 7.53–7.52 (m, 1H), 7.44–7.43 (m, 2H), 7.43–7.41 (m, 2H); HRMS (ESI-TOF) calculated for $C_{34}H_{22}O_2$ [M+Na]$^+$: 485.1510, found: 485.1512.

Scheme 2. Synthesis of lophine derivartive **6**.

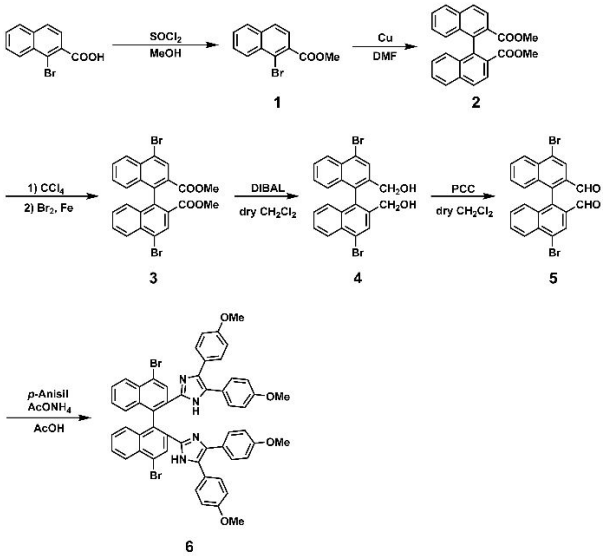

2,2′-(4,4′-Diphenyl-[1,1′-binaphthalene]-2,2′-diyl)bis(4,5-bis(4-methoxyphenyl)-imidazole) (**6-Ph**). Compound **5-Ph** (37 mg, 0.079 mmol), *p*-anisil (61 mg, 0.22 mmol), and ammonium acetate (265 mg, 2.7 mmol) were refluxed in acetic acid (2 mL) for 2 days. After cooling to room temperature, the reaction mixture was neutralized with aqueous NH_3. The slurry precipitate formed by neutralization was filtered off, washed with water, and then dried. The residue was purified by silica gel column chromatography (CH_2Cl_2/AcOEt = 5/1) to afford **6-Ph** as yellow solid (28 mg, 0.029 mmol, 37 % over 2 steps). ^{1}H NMR (400 MHz, DMSO-d_6) δ: 13.06 (s, 2H), 8.15 (s, 2H), 7.95 (d, *J* = 8.36 Hz, 2H), 7.74 (d, *J* = 7.16 Hz, 4H), 7.66 (t, *J* = 7.58 Hz, 4H), 7.61–7.54 (m, 3H), 7.46 (t, *J* = 7.10 Hz, 2H), 7.32 (t, *J* = 7.76 Hz, 2H), 7.20 (d, *J* = 8.56 Hz, 2H), 7.16 (d, *J* = 8.76 Hz, 4H), 7.02 (d, *J* = 8.72 Hz, 3H), 6.86 (d, *J* = 8.76, 4H), 6.64 (d, *J* = 8.84, 4H), 3.72 (s, 6H), 3.67 (s, 6H); HRMS (ESI-TOF) calculated for $C_{66}H_{50}N_4O_4$ [M+H]$^+$: 963.3905, found: 963.3916.

2′-(4,5-Bis(4-methoxyphenyl)imidazol-2-ylidene)-8,9-bis(4-methoxyphenyl)-4′,5-diphenyl-spiro[benzo[e]imidazo[2,1-a]isoindole-11,1′-naphthalene] (**Ph**). All manipulations were carried out with the exclusion of light. Under nitrogen, to a solution of **6-Ph** (18 mg, 0.018 mmol) in degassed benzene in benzene (10 mL) was added a solution of potassium ferricyanide (1.33 g, 3.7 mmol) and KOH (420 mg, 5.8 mmol) in water (10 mL), and the reaction mixture was vigorously stirred for 2.5 h. After the reaction was completed, the reaction product was extracted with benzene, and washed with water. The crude mixture was purified by silica gel column chromatography using AcOEt/$CHCl_3$ = 1/25 as eluent to give a red solid (1 mg, 0.001 mmol, 5 %). ^{1}H NMR (400 MHz, $CDCl_3$) δ: 8.25 (s, 1H), 7.99 (s, 1H), 7.91–7.85 (m, 1H), 7.61–7.57 (m, 1H), 7.57–7.50 (m, 7H), 7.50–7.45 (m, 5H), 7.44 (d, *J* = 8.72 Hz, 2H), 7.42–7.38 (m, 1H), 7.30 (d, *J* = 7.72 Hz, 2H), 6.84 (d, *J* = 8.68 Hz, 2H), 6.77 (d, *J* = 8.76 Hz, 2H), 6.73 (d, *J* = 8.76 Hz, 2H), 4.68 (q, *J* = 4.68, 4H), 3.81 (s, 6H), 3.75 (s, 3H) 3.73 (s, 3H); HRMS (ESI-TOF) calculated for $C_{66}H_{48}N_4O_4$ [M+H]$^+$: 961.3748, found: 961.3790.

4,4′-Bis(4-nitrophenyl)-[1,1′-binaphthalene]-2,2′-dicarbaldehyde (**5-PhNO$_2$**). Under N_2 atmosphere, compound **5** (308 mg, 0.64 mmol), $Pd(OAc)_2$ (30 mg, 0.12 mmol), dicyclohexyl(2′,6′-dimethoxy-[1,1′-biphenyl]-2-yl)phosphine (*S*Phos) (56 mg, 0.13 mmol) and Na_2CO_3 (453

Scheme 3. Synthesis of **Ph**, **PhNO$_2$** and **PhOMe**.

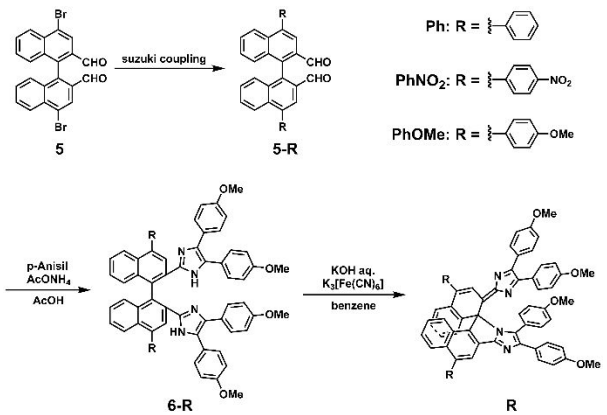

mg, 3.8 mmol) were added to degassed THF (5 mL) and water (1 mL). The mixture was stirred at 70 °C for 15.5 h. After celite filtration, the filtrate was transferred to a separation funnel and extracted with AcOEt. The organic layer was collected and the aqueous phase was extracted with AcOEt. The combined organic layers were washed with water and brine, and AcOEt was evaporated in vacuo. The crude mixture was purified by silica gel column chromatography using CH_2Cl_2/hexane = 4/1 and used in the next step without further purification.^{1}H NMR (400 MHz, $CDCl_3$) δ: 9.74 (s, 2H), 8.49 (s, 2H), 8.47 (s, 2H), 8.18 (s, 2H), 7.96 (d, *J* = 8.32 Hz, 2H), 7.84 (d, *J* = 8.72, 4H), 7.68 (t, *J* = 6.82 Hz, 2H), 7.48 (d, *J* = 5.48 Hz, 2H), 7.44 (d, *J* = 7.72 Hz, 2H); HRMS (ESI-TOF) calculated for $C_{34}H_{20}N_2O_6$ $[M+Na]^+$: 575.1214, found: 575.1190.

2,2′-(4,4′-Bis(4-nitrophenyl)-[1,1′-binaphthalene]-2,2′-diyl)bis(4,5-bis(4-methoxyphenyl)-imidazole) (**6-PhNO$_2$**). **5-PhNO$_2$** (120 mg, 0.23 mmol), *p*-anisil (189 mg, 0.64 mmol), and ammonium acetate (688 mg, 7.84 mmol) were refluxed in acetic acid (5 mL) for 12 h. After cooling to room temperature, the reaction mixture was neutralized with aqueous NH_3. The slurry precipitate formed by neutralization was filtered off, washed with water, and then dried. The residue was purified by silica gel column chromatography (CH_2Cl_2/AcOEt = 6/1) to afford 6-PhNO$_2$ as yellow solid (63 mg, 0.0723 mmol, 31 % over 2 steps). ^{1}H NMR (400 MHz, DMSO-d_6) δ: 13.01 (s, 2H), 8.52 (d, *J* = 8.72 Hz, 4H), 8.26 (s, 2H), 8.05 (d, *J* = 8.68 Hz, 4H), 7.94 (d, *J* = 7.80 Hz, 2H), 7.51 (t, *J* = 7.60 Hz, 2H), 7.36 (t, *J* = 7.76 Hz, 2H), 7.25 (d, *J* = 8.64 Hz, 2H), 7.18 (d, *J* = 8.52 Hz, 4H), 6.95 (d, *J* = 9.12 Hz, 3H), 6.87 (d, *J* = 8.56 Hz, 5H), 6.63 (d, *J* = 8.84 Hz, 4H), 3.73 (s, 6H), 3.67 (s, 6H); HRMS (ESI-TOF) calculated for $C_{66}H_{48}N_6O_8$ $[M+H]^+$: 1053.3615, found: 1053.3615.

2′-(4,5-Bis(4-methoxyphenyl)-imidazol-2-ylidene)-8,9-bis(4-methoxyphenyl)-4′,5-bis(4-nitrophenyl)-spiro[benzo[e]imidazo[2,1-a]isoindole-11,1′-naphthalene] (**PhNO$_2$**). All manipulations were carried out with the exclusion of light. Under nitrogen, to a solution of **6-PhNO$_2$** (50 mg, 0.0047 mmol) in benzene (10 mL) was added a solution of potassium ferricyanide (2.924g, 9.8 mmol) and KOH (759 mg, 15 mmol) in water (10 mL), and the reaction mixture was vigorously stirred for 8 h. After the reaction was completed, the reaction product was extracted with benzene, and washed with water. The crude mixture was purified by silica gel column chromatography using CH_2Cl_2/AcOEt = 20/1 as eluent to give red solid (1 mg, 0.072 mmol, 31 %). ^{1}H NMR (400 MHz, DMSO-d_6) δ: 8.43 (dd, *J* = 8.56 Hz, 3H), 8.15 (s, 1H), 7.88–7.83 (m, 3H), 7.78 (d, *J* = 8.40 Hz, 1H), 7.75–7.69 (m, 2H), 7.53–7.46 (m, 4H), 7.43 (dd, *J* = 9.14 Hz, 6H), 7.31 (t, *J* = 7.06 Hz, 1H), 7.25 (d, *J* = 8.00 Hz, 1H), 6.99 (d, *J* = 8.08 Hz, 1H), 6.93 (t, *J* = 8.62 Hz, 1H), 6.78 (d, *J* = 8.84 Hz, 2H), 6.72 (d, *J* = 8.64 Hz, 2H),6.44 (d, *J* = 8.56 Hz, 2H), 3.79 (s, 3H), 3.77 (s, 3H), 3.71 (s, 3H), 3.66 (s, 3H); HRMS (ESI-TOF) calculated for $C_{66}H_{46}N_6O_8$ $[M+H]^+$: 1051.3450, found: 1051.3426.

4,4′-Bis(4-methoxyphenyl)-[1,1′-binaphthalene]-2,2′-dicarbaldehyde (**5-PhOMe**). Under N_2 atmosphere, compound **5** (203 mg, 0.43 mmol), 4-methoxyphenylboronic acid (276 mg, 1.8 mmol), Na_2CO_3 (315 mg, 2.6 mmol), 2-dicyclohexylphosphino- 2′,6′-dimethoxybiphenyl (36 mg, 0.086 mmol) and palladium(II) acetate (24 mg, 0.077 mmol) were added to degassed THF (5 mL), water (1 mL) and was added. The mixture was stirred at 70 °C for 16 h. After celite filtration, the filtrate was transferred to a separation funnel and extracted with AcOEt. The organic layer was collected and the aqueous phase was extracted with AcOEt. The combined organic layers were washed with water and brine, and AcOEt was evaporated in vacuo. The crude mixture was purified by silica gel column chromatography using CH_2Cl_2/hexane = 4/1 and used in the next step without further purification. ^{1}H NMR (400 MHz, $CDCl_3$) δ: 9.73 (s, 2H), 8.14 (s, 3H), 7.57 (d, *J* = 8.68 Hz, 6H), 7.42–7.40 (m, 4H), 7.12 (d, *J* = 8.72 Hz, 6H), 3.95 (s, 6H); HRMS (ESI-TOF) calculated for $C_{36}H_{26}O_4$ $[M+Na]^+$: 545.1723, found: 545.1746.

2,2′-(4,4′-Bis(4-methoxyphenyl)-[1,1′-binaphthalene]-2,2′-diyl)bis(4,5-bis(4-methoxyphenyl)-imidazole) (**6-PhOMe**). **5-PhOMe** (15 mg, 0.040 mmol), *p*-anisil (29 mg, 0.112 mmol), and ammonium acetate (188 mg, 1.4 mmol) were refluxed in acetic acid (2 mL) for 8 h. After cooling to room temperature, the reaction mixture was neutralized with aqueous NH_3. The slurry precipitate formed by neutralization was filtered off, washed with water, and then dried. The residue was purified by silica gel column chromatography (CH_2Cl_2/AcOEt = 6/1) to afford 6-PhOMe as yellow solid (6.3 mg, 0.0072 mmol, 18 % over 2 steps). ^{1}H NMR (400 MHz, DMSO-d_6) δ: 13.21 (s, 2H), 8.07 (s, 2H), 7.98 (d, *J* = 7.96 Hz, 2H), 7.66 (d, *J* = 8.56 Hz, 4H), 7.58 (t, *J* = 7.48 Hz, 2H), 7.31 (t, *J* = 7.64 Hz, 2H), 7.21 (d, *J* = 8.64 Hz, 4H), 7.14 (dd, *J* = 8.92 Hz, 6H), 7.05 (d, *J* = 7.72 Hz, 3H), 6.85 (d, *J* = 8.92 Hz, 4H), 6.66 (dd, *J* = 5.74 Hz, 5H), 3.90 (s, 6H), 3.72 (s, 6H), 3.67 (s, 6H); HRMS (ESI-TOF) calculated for $C_{68}H_{48}N_4O_6$ $[M+H]^+$: 1023.4116, found: 1023.4108.

2′-(4,5-Bis(4-methoxyphenyl)-imidazol-2-ylidene)-4′,5,8,9-tetrakis(4-methoxyphenyl)-spiro[benzo[e]imidazo[2,1-a]isoindole-11,1′-naphthalene] (**PhOMe**). All manipulations were carried out with the exclusion of light. Under nitrogen, to a solution of **6-PhOMe** (17 mg, 0.0017 mmol) in benzene (5 mL) was added a solution of potassium ferricyanide (1.37 g, 4.06 mmol) and KOH (414 mg, 6.1 mmol) in water (5 mL), and the reaction mixture was vigorously stirred overnight. After the reaction was completed, the reaction product was extracted with benzene, and washed with water. The crude mixture was purified by preparative thin-layer chromatography (PTLC) using CH_2Cl_2/AcOEt = 20/1 as eluent to give red solid (1 mg, 0.98 μmol, 57 %).^{1}H NMR (400 MHz, $CDCl_3$) δ: 8.19 (d, *J* = 8.76 Hz,1H), 8.02 (d, *J* = 8.81 Hz,1H), 7.97 (s, 1H), 7.54 (s, 1H), 7.52 (s, 2H), 7.49–7.42 (m, 5H), 7.39–7.33 (m, 6H), 7.25–7.17 (m, 2H), 7.11 (t, *J* = 6.76 Hz, 1H), 7.04 (d, *J* = 8.80 Hz, 3H), 6.99 (d, *J* = 8.60 Hz, 2H), 6.85 (d, *J* = 8.85 Hz, 2H), 6.79 (d, *J* = 8.88 Hz, 2H), 6.73 (d, *J* = 8.92 Hz, 2H), 6.58 (d, *J* = 8.84 Hz, 2H), 6.51 (d, *J* = 8.80 Hz, 2H), 3.93 (s, 3H), 3.87 (s, 3H), 3.81 (s, 6H),3.73 (s, 3H), 3.72 (s, 3H); HRMS (ESI-TOF) calculated for $C_{68}H_{52}N_4O_6$ $[M+H]^+$: 1021.3960, found: 1021.3920.

4,4′-(2,2′-Bis(4,5-bis(4-methoxyphenyl)-imidazol-2-yl)-[1,1′-binaphthalene]-4,4′-diyl)bis(diphenylaniline) (**6-TPA**, Scheme 4). Under N_2 atmosphere, compound **6** (70 mg,

0.073 mmol), 4-(Diphenylamino)phenylboronic acid (91 mg, 0.31 mmol) $Pd(OAc)_2$ (8 mg, 0.013 mmol), dicyclohexyl(2',6'-dimethoxy-[1,1'-biphenyl]-2-yl)phosphine (*S*Phos) (13 mg, 0.0015 mmol), 4-(Diphenylamino)phenylboronic acid (92 mg, 0.31 mmol) and Na_2CO_3 (52 mg, 0.44 mmol) were added to degassed THF (5 mL) and water (1 mL). The mixture was stirred at 70 °C for 14.5 h. After celite filtration, the filtrate was transferred to a separation funnel and extracted with AcOEt. The organic layer was collected and the aqueous phase was extracted with AcOEt. The combined organic layers were washed with water and brine, and AcOEt was evaporated in vacuo. The crude sample was purified by silica gel column chromatography using CH_2Cl_2/AcOEt = 15/4 as eluent to give yellow powder (30 mg, 0.023 mmol, 32 %). ^{1}H NMR (400 MHz, DMSO-d_6) δ: 13.09 (s, 2H), 8.13 (s, 2H), 8.07 (d, *J* = 8.28 Hz, 2H), 7.66 (d, *J* = 8.32 Hz, 4H), 7.48 (t, *J* = 7.48 Hz, 3H), 7.39 (t, *J* = 7.90 Hz, 9H), 7.31 (t, *J* = 7.48 Hz, 3H), 7.21 (d, *J* = 8.48 Hz, 5H), 7.17 (d, *J* = 7.60 Hz, 11H), 7.12 (d, *J* = 7.34 Hz, 6H), 7.02 (d, *J* = 7.40 Hz, 3H), 6.84 (d, *J* = 7.04 Hz, 3H), 6.64 (d, *J* = 7.68 Hz, 3H), 3.71 (s, 6H), 3.63 (s, 6H) ; HRMS (ESI-TOF) calculated for $C_{90}H_{68}N_6O_4$ $[M+Na]^+$: 1319.5194, found: 1319.5207.

4,4'-(2'-(4,5-Bis(4-methoxyphenyl)-imidazol-2-ylidene)-8,9-bis(4-methoxyphenyl)-spiro[benzo[e]imidazo[2,1-a]isoindole-11,1'-naphthalene]-4',5-diyl)bis(diphenylaniline) (**TPA**). All manipulations were carried out with the exclusion of light. Under nitrogen, to a solution of **6-TPA** (21 mg, 0.015 mmol) in benzene (5 mL) was added a solution of potassium ferricyanide (1.108 g, 2.5 mmol) and KOH (334 mg, 6.52 mmol) in water (6 mL), and the reaction mixture was vigorously stirred overnight. After the reaction was completed, the reaction product was extracted with benzene, and washed with water. The crude mixture was purified by silica gel column chromatography using CH_2Cl_2/AcOEt = 10/1 as eluent to give reddish purple. (13 mg, 0.01 mmol, 65 %). ^{1}H NMR (400 MHz, $CDCl_3$) δ: 8.25 (s, 1H), 7.99 (s, 2H), 7.58–7.51 (m, 4H), 7.47 (t, *J* = 7.32 Hz, 4H), 7.42 (t, *J* = 9.50 Hz, 5H), 7.35–7.29 (m, 12H), 7.20 (d, *J* = 8.24 Hz, 9H), 7.17 (d, *J* = 7.08 Hz, 3H), 7.11 (d, *J* = 7.56 Hz, 2H), 7.06 (t, *J* = 7.54 Hz, 3H), 6.84 (d, *J* = 8.44 Hz, 1H), 6.77 (d, *J* = 8.56 Hz, 2H), 6.73 (d, *J* = 8.64 Hz, 2H), 6.55 (s, 3H), 3.82 (s, 3H), 3.80 (s, 3H), 3.73 (s, 3H), 3.66 (s, 3H); HRMS (ESI-TOF) calculated for $C_{90}H_{66}N_6O_4$ $[M+H]^+$: 1295.5218, found: 1295.5166.

4,4'-(2,2'-Bis(4,5-bis(4-methoxyphenyl)-imidazol-2-yl)-[1,1'-binaphthalene]-4,4'-diyl)bis(bis(4-methoxyphenyl)aniline) (**6-TPAOMe1**, Scheme 5). 4-Methoxy-(4-methoxyphenyl)-(4-(4,4,5,5-tetramethyl-1,3,2-dioxaborolan-2-yl)phenyl)aniline was synthesized according to the literature procedure.[54] Under N_2 atmosphere, compound **6** (70mg, 0.073 mmol), 4-methoxy-(4-methoxyphenyl)-(4-(4,4,5,5-tetramethyl-1,3,2-dioxaborolan-2-yl)phenyl)aniline (138 mg, 0.31 mmol), $Pd(OAc)_2$ (6 mg, 0.013 mmol), SPhos (10 mg, 0.0015 mmol) and Na_2CO_3 (50 mg, 0.44 mmol) were added to degassed THF (3 mL) and water (1 mL). The mixture was stirred at 70 °C for 10.5 h. After celite filtration, the filtrate was transferred to a separation funnel and extracted with AcOEt. The organic layer was collected and the aqueous phase was extracted with AcOEt. The combined organic layers were washed with water and brine, and AcOEt was evaporated in vacuo. This compound decomposed by using silica gel therefore it used in the next step without further purification. HRMS (ESI-TOF) calculated for $C_{94}H_{76}N_6O_8$ $[M+H]^+$: 1417.5796, found: 1417.5765.

4,4'-(2'-(4,5-Bis(4-methoxyphenyl)-imidazol-2-ylidene)-8,9-bis(4-methoxyphenyl)-spiro[benzo[e]imidazo[2,1-a]isoindole-11,1'-naphthalene]-4',5-diyl)bis(diphenylaniline) (**TPAOMe1**). All manipulations were carried out with the exclusion of light. Under nitrogen, to a solution of the crude mixture of **6-TPAOMe1** (85 mg, 0.035 mmol) in benzene (6 mL) was added a solution of potassium ferricyanide (2.40 g, 7.3 mmol) and KOH (617 mg, 11.0 mmol) in water (6 mL), and the reaction mixture was vigorously stirred overnight. After the reaction was completed, the reaction product was extracted with benzene, and washed with water. The crude mixture was purified by preparative thin-layer chromatography (PTLC) using CH_2Cl_2/AcOEt = 10/1 as eluent to give blue solid. (9 mg, 0.006 mmol, 8 % over 2 steps). ^{1}H NMR (400 MHz, $CDCl_3$) δ: 8.22 (s, 1H), 7.98 (s, 1H), 7.54–7.50 (m, 6H), 7.46 (d, *J* = 8.84 Hz, 4H), 7.43 (d, *J* = 8.76 Hz, 4H), 7.33 (d, *J* = 8.28 Hz, 5H), 7.17 (d, *J* = 2.52 Hz, 4H), 7.15 (d, *J* = 2.52 Hz, 5H), 7.02 (t, *J* = 7.82 Hz, 6H), 6.89 (t, *J* = 6.60 Hz, 9H),6.84

Scheme 4. Synthesis of **TPA**.

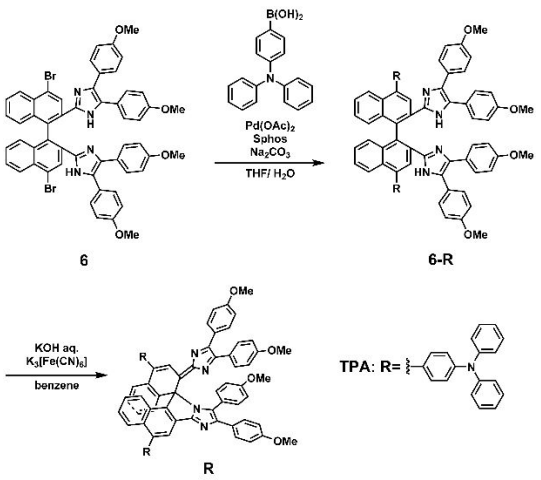

Scheme 5. Synthesis of **TPAOMe1**.

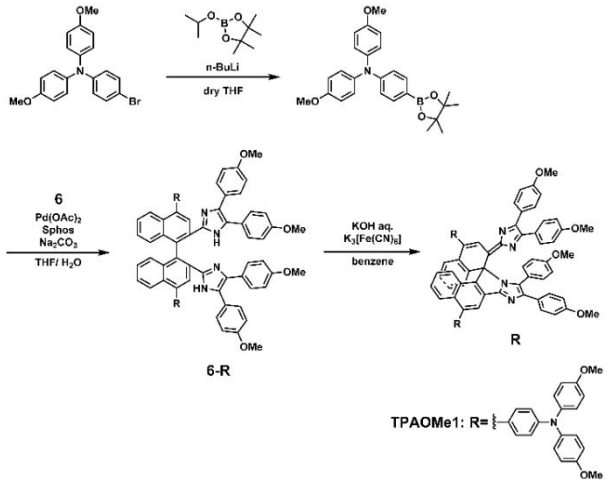

(d, *J* = 8.60 Hz, 2H), 6.76 (d, *J* = 8.60 Hz, 2H), 6.72 (d, *J* = 8.60 Hz, 2H), 6.55–6.52 (m, 3H), 3.84 (s, 6H), 3.82 (s, 6H), 3.81 (s, 3H), 3.79 (s, 3H), 3.73 (s, 3H), 3.66 (s, 3H); HRMS (ESI-TOF) calculated for $C_{94}H_{74}N_6O_8$ [M+H]$^+$: 1415.5640, found: 1415.5682.

Substitution to the imidazole unit

[1,1'-Binaphthalene]-2,2'-dicarbaldehyde was synthesized according to the literature procedure.[32] *3-Bromoperylene (**10**)* was synthesized according to the literature procedure.[55]

4-Methoxy-N-(4-methoxyphenyl)-N-phenylaniline (**7**, Scheme 6). A mixture of iodobenzene (612 mg, 3.00 mmol), 4,4'-dimethoxydiphenylamine (893 mg, 3.89 mmol), $Pd(dba)_2$ (66 mg, 0.11 mmol), Xantphos (117 mg, 0.202 mmol) and NaOtBu (450 mg, 4.68 mmol) in anhydrous degassed toluene (30 mL) and the resulting mixture was refluxed for 14 h. To the reaction mixture water and ethyl acetate were added and the mixture was extracted with ethyl acetate. The combined organic layer was washed with brine and passed through a phase separator paper. After the solvent was removed, the crude mixture was purified by silica gel column chromatography (dichloromethane/hexane = 1/1), to give desired product as an off-white solid (771 mg, yield: 84 %). ^{1}H NMR (400 MHz, $CDCl_3$) δ: 7.16 (dd, J_1 = 7.4 Hz, J_2 = 8.5 Hz, 2H), 7.04 (d, *J* = 9.0 Hz, 4H), 6.93 (d, *J* = 8.5 Hz, 2H), 6.86 (t, *J* = 7.4 Hz, 1H), 6.81 (d, *J* = 9.0 Hz, 4H), 3.79 (s, 6H); HRMS (ESI-TOF) calculated for $C_{20}H_{19}NO_2$ [M+H]$^+$: 306.1489, found: 306.1487.

1,2-Bis(4-(bis(4-methoxyphenyl)amino)phenyl)ethane-1,2-dione (**8**). A suspension of $AlCl_3$ (0.07 mL, 0.83 mmol) in dry dichloromethane (3 mL) was slowly added to a solution of **7** (504 mg, 1.65 mmol) and oxalyl chloride (0.07 mL, 0.83 mmol) in dry dichloromethane (1.5 mL) at 0 °C. The reaction mixture was stirred at ambient temperature overnight and then quenched with ice and concentrated HCl aq. After stirring for another 1 h, organic layer was passed through a phase separator paper. After the solvent was removed, the crude mixture was purified by silica gel column chromatography (ethyl acetate/dichloromethane/hexane = 3/20/20), to give desired product as a yellow solid (217 mg, 40 %). ^{1}H NMR (400 MHz, $CDCl_3$) δ: 7.72 (d, *J* = 9.0 Hz, 2H), 7.63 (d, *J* = 8.8 Hz, 2H), 7.13–7.10 (m, 8H), 6.89–6.83 (m, 10H), 6.78 (d, *J* = 9.0 Hz, 4H), 3.81 (s, 12H); HRMS (ESI-TOF) calculated for $C_{90}H_{66}N_6O_4$ [M+Na]$^+$: 687.2466, found: 687.2465.

Scheme 6. Synthesis of **TPAOMe2**.

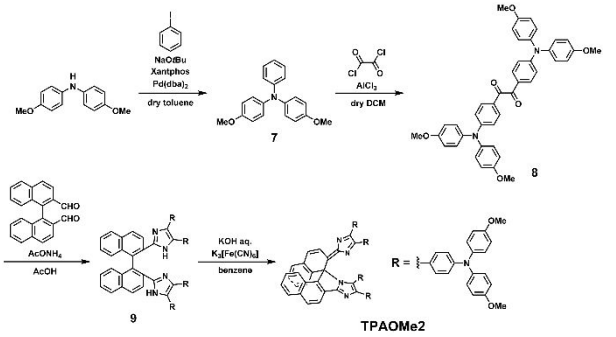

4,4',4'',4'''-([1,1'-Binaphthalene]-2,2'-diylbis(1H-imidazole-2,4,5-triyl))tetrakis(N,N-bis(4-methoxyphenyl)aniline) (**9**). [1,1'-binaphthalene]-2,2'-dicarbaldehyde (21 mg, 0.068 mmol), **8** (99 mg, 0.15 mmol), and ammonium acetate (284 mg, 3.68 mmol) were refluxed in AcOH (5 mL) for 15 h. After cooling to room temperature, the reaction mixture was neutralized with aqueous NH_3 and extracted with chloroform. The combined organic layer was washed with water and brine and passed through a phase separator paper. After the solvent was removed, the crude mixture was purified by triethyl amine treated silica gel column chromatography (ethyl acetate/dichloromethane/hexane = 3/10/10), to give desired product as a pale yellow solid (31 mg, 29 %). ^{1}H NMR (400 MHz, DMSO-d_6) δ: 13.74 (s, 2H), 8.12 (d, *J* = 8.5 Hz, 2H), 7.99 (d, *J* = 8.3 Hz, 2H), 7.92 (d, *J* = 8.5 Hz, 2H), 7.44 (t, *J* = 7.7 Hz, 2H), 7.24 (t, *J* = 7.7 Hz, 2H), 7.08 (d, *J* = 8.7 Hz, 4H), 7.01–6.81 (m, 38H), 6.59–6.53 (m, 8H), 3.70 (s, 12H), 3.69 (s, 12H); HRMS (ESI-TOF) calculated for $C_{106}H_{86}N_8O_8$ [M+H]+: 1599.6641, found: 1599.6597.

4,4'-(2-(8,9-bis(4-(bis(4-methoxyphenyl)amino)phenyl)-2'H-spiro[benzo[e]imidazo[2,1-a]isoindole-11,1'-naphthalen]-2'-ylidene)-2H-imidazole-4,5-diyl)bis(N,N-bis(4-methoxyphenyl)aniline) (**TPAOMe2**). To a solution of **9** (27 mg, 0.017 mmol) in benzene (2 mL) was added a solution of potassium ferricyanide (167 mg, 0.51 mmol) and KOH (71 mg, 1.3 mmol) in water (2.5 mL), and the reaction mixture was vigorously stirred overnight. The organic layer was separated, exhaustively washed with water and passed through a phase separator paper. After the solvent was removed, the crude mixture was purified by triethyl amine treated silica gel column chromatography (THF/benzene = 1/200 → 1/40), to give desired product as a dark blue solid (17 mg, 63 %). ^{1}H NMR (400 MHz, DMSO-d_6) δ: 8.10 (d, *J* = 8.6 Hz, 1H), 8.01 (d, *J* = 8.6 Hz, 1H), 7.94 (d, *J* = 7.8 Hz, 1H), 7.86 (d, *J* = 9.8 Hz, 1H), 7.44 (d, *J* = 7.5 Hz, 1H), 7.37–7.26 (m, 10H), 7.21 (d, *J* = 10.0 Hz, 1H), 7.09 (t, *J* = 7.8 Hz, 10H), 6.99–6.87 (m, 26H), 6.70 (d, *J* = 7.8 Hz, 1H), 6.62–6.59 (m, 4H), 8.50 (d, *J* = 9.0 Hz, 1H), 6.40 (d, *J* = 8.6 Hz, 1H), 6.17 (d, *J* = 8.6 Hz, 1H), 3.73 (m, 18H), 3.72 (s, 6H); HRMS (ESI-TOF) calculated for $C_{106}H_{84}N_8O_8$ [M+H]$^+$: 1598.6517, found: 1598.6601.

N,N-Bis(4-methoxyphenyl)perylen-3-amine (**11**, Scheme 7). A mixture of 3-bromoperylene (404 mg, 1.09 mmol), 4,4'-dimethoxydiphenylamine (594 mg, 2.59 mmol), $Pd_2(dba)_3$ (72 mg, 0.079 mmol), $P(tBu)_3$ (76 mg, 0.31 mmol) and NaOtBu (340 mg, 3.54 mmol) in dry toluene (53 mL) was stirred under a nitrogen atmosphere at 110 °C for 12 h. The reaction mixture was filtered through a Celite pad and washed with brine. The organic layer was passed through a phase separator paper. After the solvent was removed, the crude mixture was purified by silica gel column chromatography (dichloromethane/hexane = 3/2), to give desired product as a yellow solid (359 mg, 68 %). ^{1}H NMR (400 MHz, $CDCl_3$) δ: 8.18–8.11 (m, 4H), 7.83 (d, *J* = 8.4 Hz, 1H), 7.67 (t, *J* = 8.4 Hz, 2H), 7.50–7.45 (m, 2H), 7.34 (t, *J* = 7.9 Hz, 1H), 7.20 (d, *J* = 7.9 Hz, 1H), 6.98 (d, *J* = 8.9 Hz,

4H), 6.78 (d, *J* = 8.9 Hz, 4H), 3.77 (s, 6H); HRMS (ESI-TOF) calculated for $C_{34}H_{25}NO_2$ $[M+H]^+$: 480.1958, found: 480.1948.

10-Bromo-N,N-bis(4-methoxyphenyl)perylen-3-amine (**12**). A solution of *N*-bromosuccinimide (NBS) (165 mg, 0.93 mmol) in dry THF (30 mL) was added to a solution of **11** (304 mg, 0.63 mmol) in dry THF (120 mL) and stirred at 0 °C under nitrogen atmosphere for 30 min. The mixture was poured into water and extracted with dichloromethane. The organic layer was passed through a phase separator paper and the solvent was removed, the residue was purified by silica gel column chromatography (dichloromethane/hexane = 3/2), to give desired product as a red solid (228 mg, 64 %). ^{1}H NMR (400 MHz, $CDCl_3$) δ: 8.23 (d, *J* = 8.0 Hz, 1H), 8.18 (d, *J* = 8.0 Hz, 1H), 8.12 (d, *J* = 8.4 Hz, 1H), 8.09 (d, *J* = 8.0 Hz, 1H), 7.94 (d, *J* = 8.3 Hz, 1H), 7.86 (d, *J* = 8.0 Hz, 1H), 7.76 (d, *J* = 8.3 Hz, 1H), 7.59 (t, *J* = 8.0 Hz, 1H), 7.35 (t, *J* = 8.0 Hz, 1H), 7.19 (d, *J* = 8.4 Hz, 1H), 6.97 (d, *J* = 9.0 Hz, 4H), 6.78 (d, *J* = 9.0 Hz, 4H), 3.77 (s, 6H); HRMS (ESI-TOF) calculated for $C_{34}H_{24}NO_2Br$ $[M+H]^+$: 557.0985, found: 557.1010.

10-((4-(Tert-butyl)phenyl)ethynyl)-N,N-bis(4-methoxyphenyl)perylen-3-amine (**13**). Compound **12** (107 mg, 0.19 mmol), CuI (32 mg, 0.17 mmol) and $Pd(PPh_3)_2Cl_2$ (57 mg, 0.081 mmol) were weighed into a Schlenk tube under nitrogen atmosphere. A mixture of piperidine (3 mL, 30.3 mmol) and 1,4-dioxane (8 mL) containing 4-*tert*-butylphenylacetylene (0.1 mL, 0.56 mmol) were purged with nitrogen before syringed into the tube. The resulting solution was stirred at 105 °C overnight. The reaction mixture was quenched with saturated aqueous NH_4Cl and extracted with dichloromethane. The combined organic layer was washed with water and passed through a phase separator paper. After the solvent was removed, the crude mixture was purified by silica gel column chromatography (dichloromethane/hexane = 3/2), to give desired product as a dark red solid (86 mg, 71 %). ^{1}H NMR (400 MHz, $CDCl_3$) δ: 8.31 (d, *J* = 8.2 Hz, 1H), 8.24 (d, *J* = 7.6 Hz, 1H), 8.19 (d, *J* = 8.0 Hz, 1H), 8.14 (d, *J* = 8.1 Hz, 1H), 8.08 (d, *J* = 7.9 Hz, 1H), 7.84 (d, *J* = 8.0 Hz, 1H), 7.73 (d, *J* = 7.9 Hz, 1H), 7.61–7.58 (m, 3H), 7.43 (d, *J* = 8.2 Hz, 2H), 7.35 (t, *J* = 8.0 Hz, 1H), 7.21 (d, *J* = 8.1 Hz, 1H), 6.98 (d, *J* = 8.9 Hz, 4H), 6.78 (d, *J* = 8.9 Hz, 4H), 3.78 (s, 6H), 1.36 (s, 9H); HRMS (ESI-TOF) calculated for $C_{46}H_{37}NO_2$ $[M+H]^+$: 636.2897, found: 636.2874.

1-(10-(Bis(4-methoxyphenyl)amino)perylen-3-yl)-2-(4-(tert-butyl)phenyl)ethane-1,2-dione (**14**). The mixture of **13** (77 mg, 0.12 mmol) and $PdCl_2$ (89 mg, 0.50 mmol) in DMSO (9 mL) was stirred at 140 °C overnight. The reaction mixture was diluted with water and extracted with dichloromethane. The combined organic layer was washed with water and passed through a phase separator paper. After the solvent was removed, the crude mixture was purified by silica gel column chromatography (dichloromethane), to give desired product as a dark purple solid (56 mg, 69 %). ^{1}H NMR (400 MHz, $CDCl_3$) δ: 9.33 (d, *J* = 8.0 Hz, 1H), 8.35 (d, *J* = 8.0 Hz, 1H), 8.28 (d, *J* = 7.6 Hz, 1H), 8.19 (d, *J* = 8.4 Hz, 1H), 8.04 (d, *J* = 8.0 Hz, 1H), 7.99 (d, *J* = 8.4 Hz, 2H), 7.89 (d, *J* = 7.6 Hz, 1H), 7.87 (d, *J* = 8.0 Hz, 1H), 7.76 (t, *J* = 8.0 Hz, 1H), 7.54 (d, *J* = 8.4 Hz, 2H), 7.38 (t, *J* = 7.6 Hz, 1H), 7.19 (d, *J* = 8.4 Hz, 1H), 6.97 (d, *J* = 9.0 Hz, 4H), 6.79 (d, *J* = 9.0 Hz, 4H), 3.78 (s, 6H), 1.35 (s, 9H); HRMS (ESI-TOF) calculated for $C_{46}H_{37}NO_4$ $[M+Na]^+$: 690.2615, found: 590.2617.

APery. [1,1'-Binaphthalene]-2,2'-dicarbaldehyde (16 mg, 0.052 mmol), **14** (50 mg, 0.075 mmol), and ammonium acetate (301 mg, 3.9 mmol) were refluxed in acetic acid (7 mL) for 25.5 h. After cooling to room temperature, the reaction mixture was neutralized with aqueous NH_3 and extracted with dichloromethane. The combined organic layer was washed with water and brine and passed through a phase separator paper. After the solvent was removed, the crude mixture was purified by triethyl amine treated silica gel column chromatography (dichloromethane/hexane = 7/3), to give a mixture of the structural isomers of lophine presursors (**15**) as a dark red solid (38 mg, 63 %) which was used for the next step without further purification. The product was identified by HRMS, (ESI-TOF) calcd for $C_{114}H_{88}N_6O_4$ $[M+Na]^+$: 1627.6759, found: 1627.6718.

Under nitrogen, to a solution of **15** (34 mg, 0.021 mmol) in benzene (20 mL) was added a solution of potassium ferricyanide (3.75 g, 11.4 mmol) and KOH (858 mg, 15.3 mmol) in water (20 mL), and the reaction mixture was vigorously stirred overnight. The organic layer was separated, exhaustively washed with water and passed through a phase separator paper. After the solvent was removed, the crude mixture was purified by triethyl amine treated silica gel column chromatography (dichloromethane/hexane = 4/1), to give a mixture of the structural isomers of desired product (20 mg, 59 %) as a black solid. One of the structural isomers was isolated by

Scheme 7. Synthesis of **APery**.

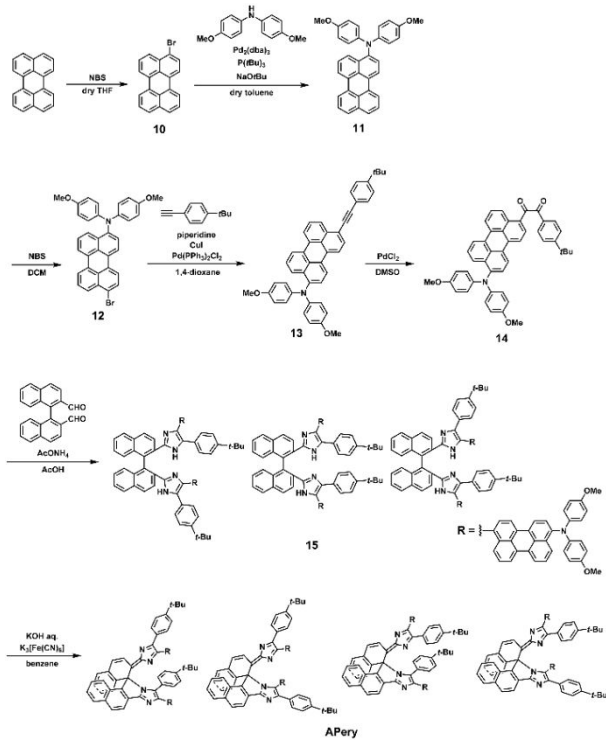

high performance liquid chromatography (MeCN/THF = 5/1). ^{1}H NMR (400 MHz, DMSO-d_6) δ: 8.10 (d, J = 8.6 Hz, 1H), 8.01 (d, J = 8.6 Hz, 1H), 7.94 (d, J = 7.8 Hz, 1H), 7.86 (d, J = 9.8 Hz, 1H), 7.44 (d, J = 7.5 Hz, 1H), 7.37–7.26 (m, 10H), 7.21 (d, J = 10.0 Hz, 1H), 7.09 (t, J = 7.8 Hz, 10H), 6.99–6.87 (m, 26H), 6.70 (d, J = 7.8 Hz, 1H), 6.62–6.59 (m, 4H), 8.50 (d, J = 9.0 Hz, 1H), 6.40 (d, J = 8.6 Hz, 1H), 6.17 (d, J = 8.6 Hz, 1H), 3.73 (m, 18H), 3.72 (s, 6H); HRMS (ESI-TOF) calculated for $C_{114}H_{86}N_6O_4$ $[M+H]^+$: 1603.6783, found: 1603.6801.

ASSOCIATED CONTENT

Supporting Information

NMR spectra, ESI-TOF-MS spectra, HPLC charts and the other experimental details (PDF). This material is available free of charge via the Internet at http://pubs.acs.org.

AUTHOR INFORMATION

Corresponding Author

*jiro_abe@chem.aoyama.ac.jp

Author Contributions

The manuscript was written through contributions of all authors.

Notes

Any additional relevant notes should be placed here.

ACKNOWLEDGMENT

This work was supported by JSPS KAKENHI Grant Number JP18H05263.

REFERENCES

(1) Irie, M.; Fukaminato, T.; Matsuda K.; Kobatake, S. Photochromism of Diarylethene Molecules and Crystals: Memories, Switches, and Actuators. *Chem. Rev.* **2014**, *114* (24), 12174–12277.

(2) Balzani, V.; Credi, A.; Raymo, F. M.; Stoddart, J. F. Artificial Molecular Machines. *Angew. Chem., Int. Ed.* **2000**, *39* (19), 3348–3391.

(3) Feringa, B. L.; Browne, W. R. *Molecular Switches*; Wiley-VCH: Weinheim, Germany, 2011.

(4) Yokoyama, Y.; Nakatani, K. *Photon-Working Switches*; Springer: Tokyo, 2017.

(5) Crano, J. C.; Guglielmetti, R. J. *Organic Photochromic and Thermochromic Compounds*; Plenum Press: New York, 1999.

(6) Kuroiwa, H.; Inagaki, Y.; Mutoh, K.; Abe, J. On-Demand Control of the Photochromic Properties of Naphthopyrans. *Adv. Mater.* **2019**, *31* (2), 1805661.

(7) Deniz, E.; Tomasulo, M.; Cusido, J.; Sortino, S.; Raymo, F. M. Fast and Stable Photochromic Oxazines for Fluorescence Switching. *Langmuir* **2011**, *27* (19), 11773–11783.

(8) Mutoh, K.; Sliwa, M.; Abe, J. Rapid Fluorescence Switching by Using a Fast Photochromic [2.2]Paracyclophane-Bridged Imidazole Dimer. *J. Phys. Chem. C* **2013**, *117* (9), 4808–4814.

(9) Ishii. N.; Kato, T.; Abe, J. A Real-Time Dynamic Holographic Material Using a Fast Photochromic Molecule. *Sci. Rep.* **2012**, *2*, 819.

(10) Kobayashi, Y.; Abe, J. Real-Time Dynamic Hologram of a 3D Object with Fast Photochromic Molecules. *Adv. Optical Mater.* **2016**, *4* (9), 1354–1357.

(11) Ernst, O. P.; Lodowski, D. T.; Elstner, M.; Hegemann, P.; Brown, L. S.; Kandori, H. Microbial and Animal Rhodopsins: Structures, Functions, and Molecular Mechanisms. *Chem. Rev.* **2014**, *114* (1) 126–163.

(12) Tsuboi, Y.; Shimizu, R.; Shoji, T.; Kitamura, N. Near-Infrared Continuous-Wave Light Driving a Two-Photon Photochromic Reaction with the Assistance of Localized Surface Plasmon. *J. Am. Chem. Soc.* **2009**, *131* (35), 12623–12627.

(13) Boyer, J.-C.; Carling, C.-J.; Gates, B. D.; Branda, N. R. Two-Way Photoswitching Using One Type of Near-Infrared Light, Upconverting Nanoparticles, and Changing Only the Light Intensity. *J. Am. Chem. Soc.* **2010**, *132* (44), 15766–15772.

(14) Yan, B.; Boyer, J.-C.; Branda, N. R.; Zhao, Y. Near-Infrared Light-Triggered Dissociation of Block Copolymer Micelles Using Upconverting Nanoparticles. *J. Am. Chem. Soc.* **2011**, *133* (49), 19714–19717.

(15) Mori, K.; Ishibashi, Y.; Matsuda, H.; Ito, S.; Nagasawa, Y.; Nakagawa, H.; Uchida, K.; Yokojima, S.; Nakamura, S.; Irie, M.; Miyasaka, H. One-Color Reversible Control of Photochromic Reactions in a Diarylethene Derivative: Three-Photon Cyclization and Two-Photon Cycloreversion by a Near-Infrared Femtosecond Laser Pulse at 1.28 μm. *J. Am. Chem. Soc.* **2011**, *133* (8), 2621–2625.

(16) Kobayashi, Y.; Katayama, T.; Yamane, T.; Setoura, K.; Ito, S.; Miyasaka, H.; Abe, J. Stepwise Two-Photon-Induced Fast Photoswitching via Electron Transfer in Higher Excited States of Photochromic Imidazole Dimer. *J. Am. Chem. Soc.*, **2016**, *138* (18), 5930–5938.

(17) Tokunaga, A.; Martinez, L.; Mutoh, K.; Fron, E.; Hofkens, J.; Sliwa, M.; Abe, J. Photochromic Reaction by Red Light via Triplet Fusion Upconversion. *J. Am. Chem. Soc.*, **2019**, *141* (44), 17744–17753.

(18) Mi, Y.; Cheng, H.-B.; Chu, H.; Zhao, J.; Yu, M.; Gu, Z.; Zhao, Y.; Li, L. A Photochromic Upconversion Nanoarchitecture: Towards Activatable Bioimaging and Dual NIR Light-Programmed Singlet Oxygen Generation. *Chem. Sci.*, **2019**, *10* (44), 10231–10239.

(19) Bléger, D.; Hecht, S. Visible-Light-Activated Molecular Switches. *Angew. Chem. Int. Ed.* **2015**, *54* (39), 11338–11349.

(20) Hemmer, J. R.; Poelma, S. O.; Treat, N.; Page, Z. A.; Dolinski, N. D.; Diaz, Y. J.; Tomlinson, W.; Clark, K. D.; Hooper, J. P.; Hawker, C.; Read De Alaniz, J. Tunable Visible and Near Infrared Photoswitches. *J. Am. Chem. Soc.* **2016**, *138* (42), 13960–13966.

(21) Hemmer, J. R.; Page, Z. A.; Clark, K. D.; Stricker, F.; Dolinski, N. D.; Hawker, C. J.; Read De Alaniz, J. Controlling Dark Equilibria and Enhancing Donor-Acceptor Stenhouse Adduct Photoswitching Properties through Carbon Acid Design. *J. Am. Chem. Soc.* **2018**, *140* (33), 10425–10429.

(22) Klaue, K.; Garmshausen, Y.; Hecht, S. Taking Photochromism beyond Visible: Direct One-Photon NIR Photoswitches Operating in the Biological Window. *Angew. Chem. Int. Ed.* **2018**, *57* (5), 1414–1417.

(23) Lentes, P.; Stadler, E.; Röhricht, F.; Brahms, A.; Gröbner, J.; Sönnichsen, F. D.; Gescheidt, G.; Herges, R. Nitrogen Bridged Diazocines: Photochromes Switching within the Near-Infrared Region with High Quantum Yields in Organic Solvents and in Water. *J. Am. Chem. Soc.* **2019**, *141* (34), 13592–13600.

(24) Shimizu, I.; Kokado, H.; Inoue, E. Photoreversible Photographic Systems. VI. Reverse Photochromism of 1,3,3-Trimethylspiro[indoline-2,2′-benzopyran]-8′-carboxylic Acid. *Bull. Chem. Soc. Jpn.* **1969**, *42* (6), 1730–1734.

(25) Sunamoto, J.; Iwamoto, K.; Akutagawa, M.; Nagase, M.; Kondo, H. Rate Control by Restricting Mobility of Substrate in Specific Reaction Field. Negative Photochromism of Water-Soluble Spiropyran in AOT Reversed Micelles. *J. Am. Chem. Soc.* **1982**, *104* (18), 4904–4907.

(26) Ciardelli, F.; Fabbri, D.; Pieroni, O.; Fissi, A. Photomodulation of Polypeptide Conformation by Sunlight in Spiropyran-Containing Poly(L-glutamic acid). *J. Am. Chem. Soc.* **1989**, *111* (9), 3470–3472.

(27) Tanaka, M.; Nakamura, M.; Salhin, M. A. A.; Ikeda, T.; Kamada, K.; Ando, H.; Shibutani, Y.; Kimura, K. Synthesis and Photochromism of Spirobenzopyran Derivatives Bearing an Oxymethylcrown Ether Moiety: Metal Ion-Induced Switching between Positive and Negative Photochromisms. *J. Org. Chem.* **2001**, *66* (5), 1533–1537.

(28) Blattmann, H.-R.; Meuche, D.; Heilbronner, E.; Molyneux, R. J.; Boekelheide, V. Photoisomerization of *trans*-15,16-Dimethyldihydropyrene. *J. Am. Chem. Soc.* **1965**, *87* (1), 130–131.

(29) Mitchell, R. H.; The Metacyclophanediene-Dihydropyrene Photochromic π Switch. *Eur. J. Org. Chem.* **1999**, (11), 2695–2703.

(30) Honda, K.; Komizu, H.; Kawasaki, M. Reverse Photochromism of Stenhouse Salts. *J. Chem. Soc., Chem. Commun.* **1982**, 253–254.

(31) Helmy, S.; Leibfarth, F. A.; Oh, S.; Poelma, J. E.; Hawker, C. J.; Read de Alaniz, J. Photoswitching Using Visible Light: A New Class of Organic Photochromic Molecules. *J. Am. Chem. Soc.* **2014**, *136* (23), 8169–8172.

(32) Hatano, S.; Horino, T.; Tokita, A.; Oshima, T.; Abe, J. Unusual Negative Photochromism via a Short-Lived Imidazolyl Radical of 1,1′-Binaphthyl-Bridged Imidazole Dimer. *J. Am. Chem. Soc.* **2013**, *135* (8), 3164–3172.

(33) Yonekawa, I.; Mutoh, K.; Kobayashi, Y.; Abe, J. Intensity-Dependent Photoresponse of Biphotochromic Molecule Composed of a Negative and a Positive Photochromic Unit. *J. Am. Chem. Soc.* **2018**, *140* (3), 1091–1097.

(34) Yonekawa, I.; Mutoh, K.; Abe, J. Visible Light Intensity Dependent Negative Photochromism of Binaphthyl-Bridged Phenoxyl-Imidazolyl Radical Complex. *Chem. Commun.* **2019**, 55 (9), 1221–1224.

(35) Mutoh, K.; Miyashita, N.; Arai, K.; Abe, J. Turn-On Mode Fluorescence Switch by Using Negative Photochromic Imidazole Dimer. *J. Am. Chem. Soc.* **2019**, *141* (14), 5650–5654.

(36) Yamaguchi, T.; Kobayashi Y.; Abe, J. Fast Negative Photochromism of 1,1'-Binaphthyl-Bridged Phenoxyl-Imidazolyl Radical Complex. *J. Am. Chem. Soc.* **2016**, *138* (3), 906–913.

(37) Mutoh, K.; Kobayashi, Y.; Hirao, Y.; Kubo, T.; Abe, J. Stealth Fast Photoswitching of Negative Photochromic Naphthalene-Bridged Phenoxyl-Imidazolyl Radical Complexes. *Chem. Commun.* **2016**, 52 (41), 6797–6800.

(38) Tian, H.; Zhang, J. *Photochromic Materials*; Wiley-VCH: Weinheim, Germany, 2016.

(39) Klessinger, M.; Michl, J. *Excited States and Photochemistry of Organic Molecules*; VCH-Publisher: New York, USA, 1995.

(40) Minkin, V. I. Photo-, Thermo-, Solvato-, and Electrochromic Spiroheterocyclic Compounds. *Chem. Rev.* 2004, *104* (5), 2751–2776.

(41) Satoh, Y.; Ishibashi, Y.; Ito, S.; Nagasawa, Y.; Miyasaka, H.; Chosrowjan, H.; Taniguchi, S.; Mataga, N.; Kato, D.; Kikuchi, A.; Abe, J. Ultrafast Laser Photolysis Study on Photodissociation Dynamics of a Hexaarylbiimidazole Derivative. *Chem. Phys. Lett.* **2007**, *448* (4), 228–231.

(42) Miyasaka, H.; Satoh, Y.; Ishibashi, Y.; Ito, S.; Taniguchi, S.; Chosrowjan, H.; Mataga, N.; Kato, D.; Kikuchi, A.; Abe, J. Ultrafast Photodissociation Dynamics of a Hexaarylbiimidazole Derivative with Pyrenyl Groups. Dispersive Reaction from Femtosecond to 10 ns Time Regions. *J. Am. Chem. Soc.* **2009**, *131* (21), 7256–7263.

(43) Mutoh, K.; Nakano, E.; Abe, J. Spectroelectrochemistry of a Photochromic [2.2]Paracyclophane-Bridged Imidazole Dimer: Clarification of the Electrochemical Behavior of HABI. *J. Phys. Chem. A* **2012**, *116* (25), 6792–6797.

(44) Yamamoto, K.; Mutoh, K.; Abe, J. Photo- and Electro-Driven Molecular Switching System of Aryl-Bridged Photochromic Radical Complexes. *J. Phys. Chem. A* **2019**, *123* (10), 1945–1952.

(45) Song, L.; Yang, Y.; Zhang, Q.; Tian, H.; Zhu, W.-H. Synthesis and Photochromism of Naphthopyrans Bearing Naphthalimide Chromophore: Predominant Thermal Reversibility in Color-Fading and Fluorescence Switch. *J. Phys. Chem. B* **2011**, *115* (49), 14648–14658.

(46) Yamashita, H.; Abe, J. Photochromic Properties of [2.2]Paracyclophane-Bridged Imidazole Dimer with Increased Photosensitivity by Introducing Pyrenyl Moiety. *J. Phys. Chem. A* **2011**, *115* (46), 13332–13337.

(47) Wu, Y.; Guo, Z.; Zhu, W.-H. Wan, W.; Zhang, J.; Li, W.; Li, X.; Tian, H.; Li, A. D. Q. Photoswitching Between Black and Colourless Spectra Exhibits Resettable Spatiotemporal Logic. *Mater. Horiz.* **2016**, *3* (2), 124–129.

(48) Hanazawa, M.; Sumiya, R.; Horikawa, Y.; Irie, M. Thermally Irreversible Photochromic Systems. Reversible Photocyclization of 1,2-Bis(2-methylbenzo[*b*]thiophen-3-yl)perfluorocyclocoalkene Derivatives. *J. Chem. Soc., Chem. Commun.* **1992**, (3), 206–207.

(49) Yamaguchi, T.; Uchida, K.; Irie, M. Photochromic Properties of Diarylethene Derivatives Having Benzofuran and Benzothiophene Rings Based on Regioisomers. *Bull. Chem. Soc. Jpn.* **2008**, *81* (5), 644–652.

(50) McMurry, J. E. Fay, R. C. *General Chemistry: Atoms First 2nd Ed.*; Pearson: Tokyo, 2013.

(51) Seki, M.; Yamada, S.; Kuroda, T.; Imashiro, R; Shimizu, T. A Practical Synthesis of C_2-Symmetric Chiral Binaphthyl Ketone Catalyst. *Synthesis*. **2000**, (12), 1677–1680.

(52) Kim, J.; Schuster, G. B. Enantioselective Catalysis of the Triplex Diels-Alder Reaction: a Study of Scope and Mechanism. *J. Am. Chem. Soc.*, **1992,** *114* (24), 9309–9317.

(53) Abe, M.; Ohmori, M.; Suzuki, K.; Yamamoto, T. Synthesis and Chiroptical Properties of π-Conjugated Polymer Consisting of Dihydropentahelicene Units with Axial Chirality. *Journal of Polymer Science*. **2010**, *48* (8), 1844–1848.

(54) Teng, C, Yang, X.; Yang, C.; Li, S.; Cheng, M.; Hagfeldt, A.; Sun, L. Molecular Design of Anthracene-Bridged Metal-Free Organic Dyes for Efficient Dye-Sensitized Solar Cells. *J. Phys. Chem. C* **2010,** *114* (19), 9101–9110.

(55) Karikachey, A. R.; Lee, H. B.; Masjedi, M.; Ross, A.; Moody, M. A.; Cai, X.; Chui, M.; Hoff, C. D.; Sharp, P. R. High Quantum Yield Molecular Bromine Photoelimination from Mononuclear Platinum(IV) Complexes. *Inorg. Chem.*, **2013**, *52* (7), 4113–4119.

Insert Table of Contents artwork here

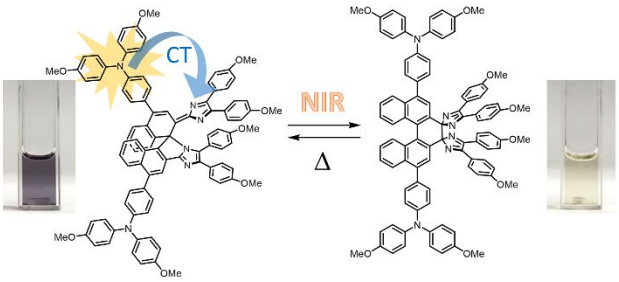

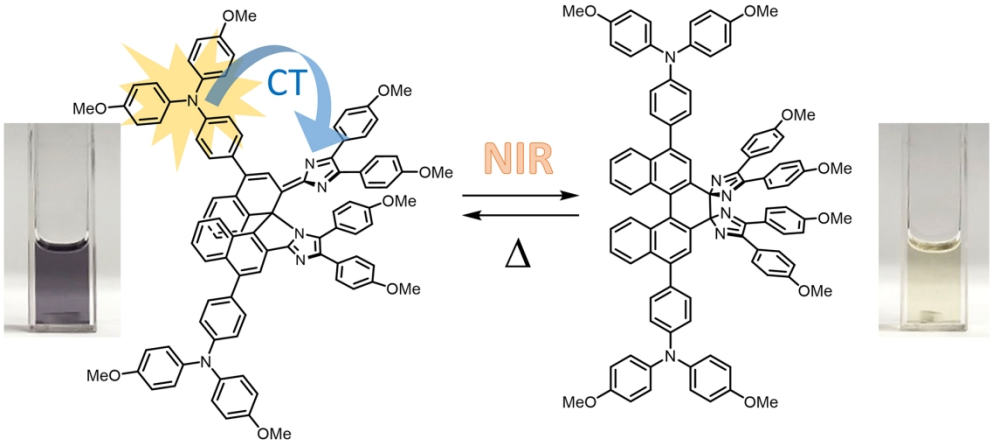

82x37mm (600 x 600 DPI)

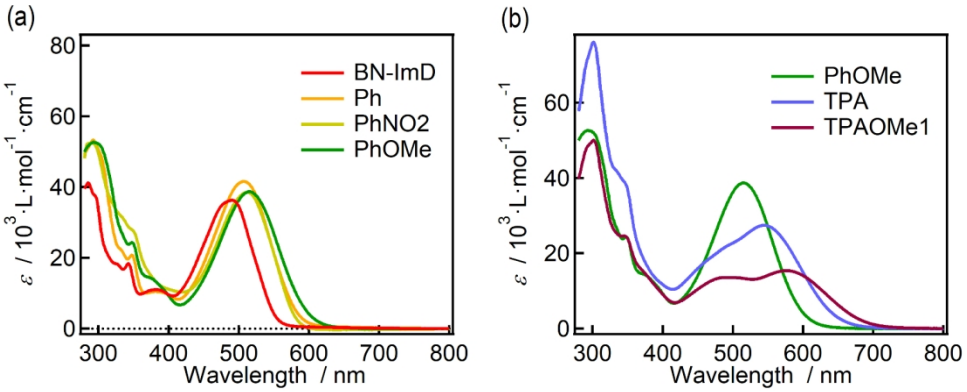

78x33mm (594 x 594 DPI)

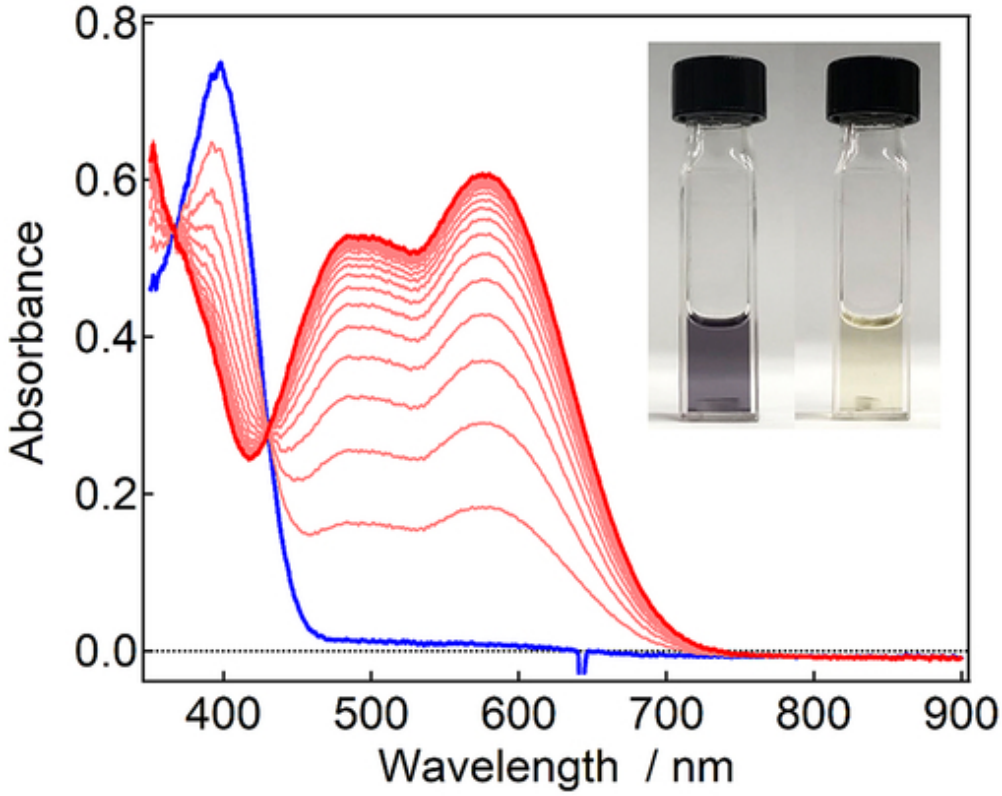

Figure 2

43x34mm (300 x 300 DPI)

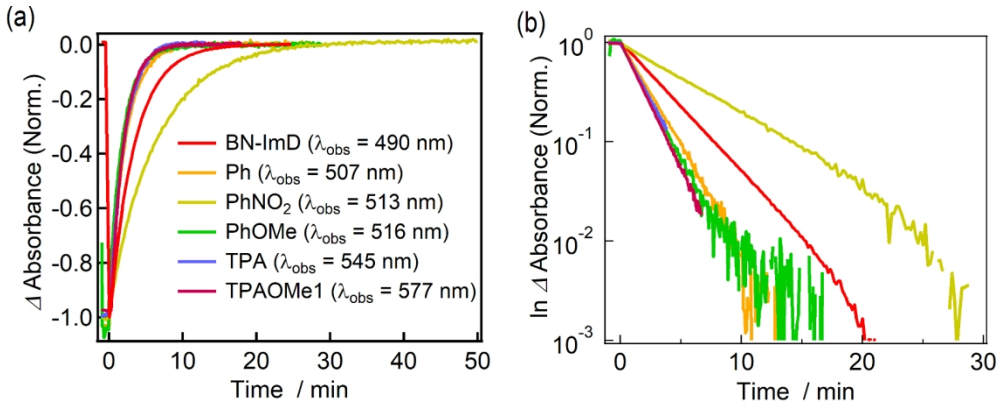

78x31mm (594 x 594 DPI)

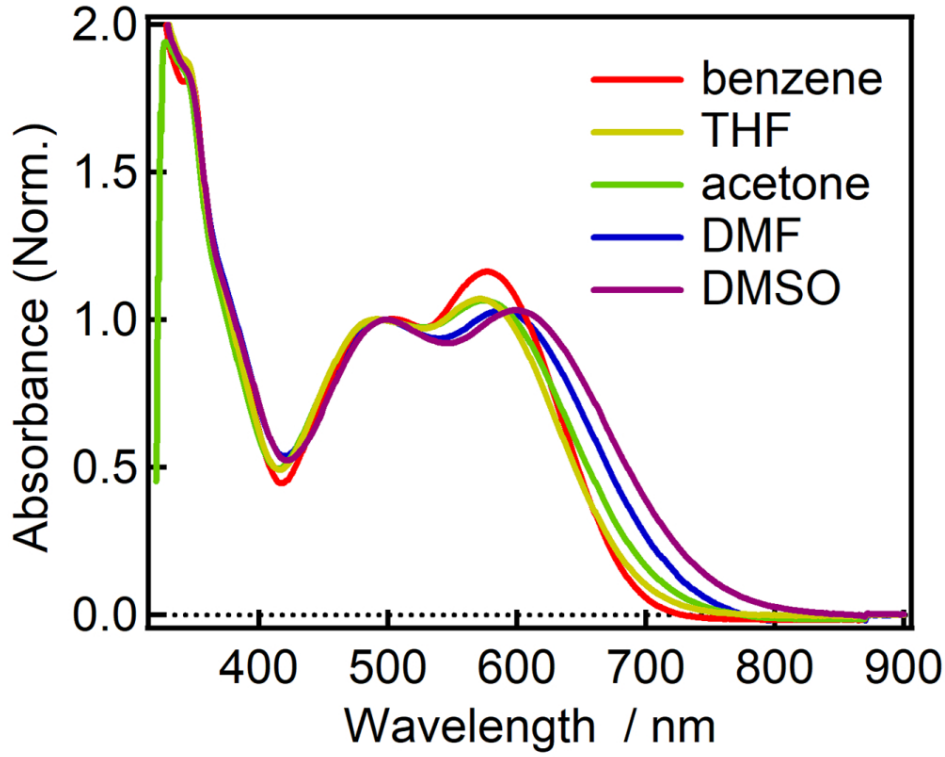
2.0
1.5
1.0
0.5
0.0
Absorbance (Norm.)
400
500
600
700
800
900
Wavelength / nm
benzene
THF
acetone
DMF
DMSO

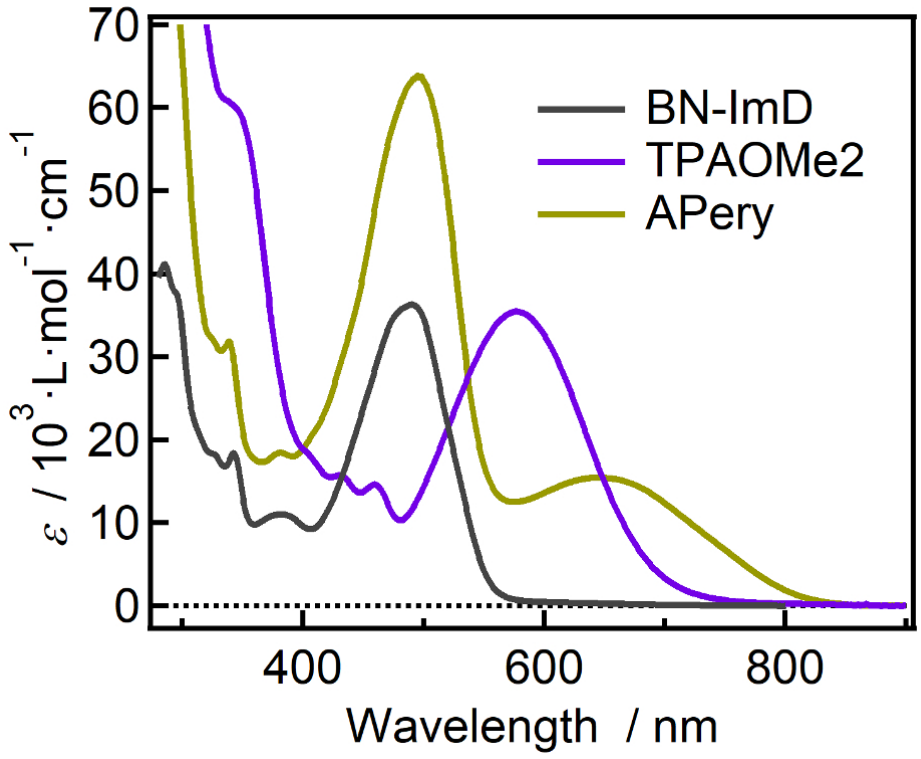

42x34mm (594 x 594 DPI)

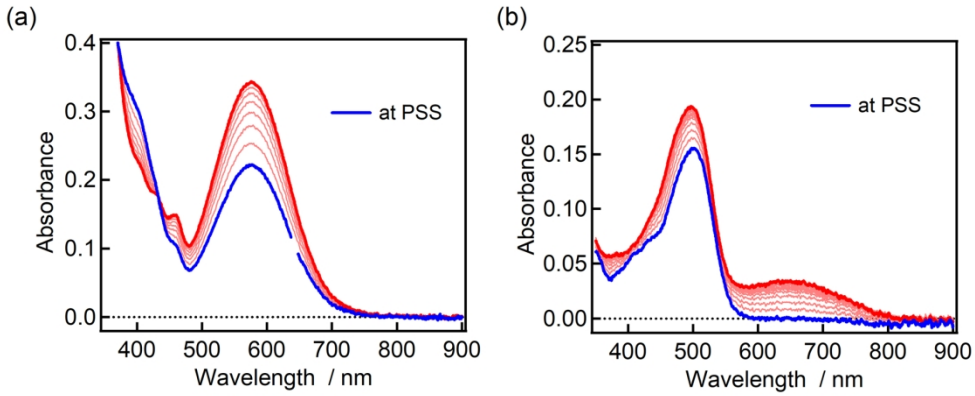

80x33mm (600 x 600 DPI)

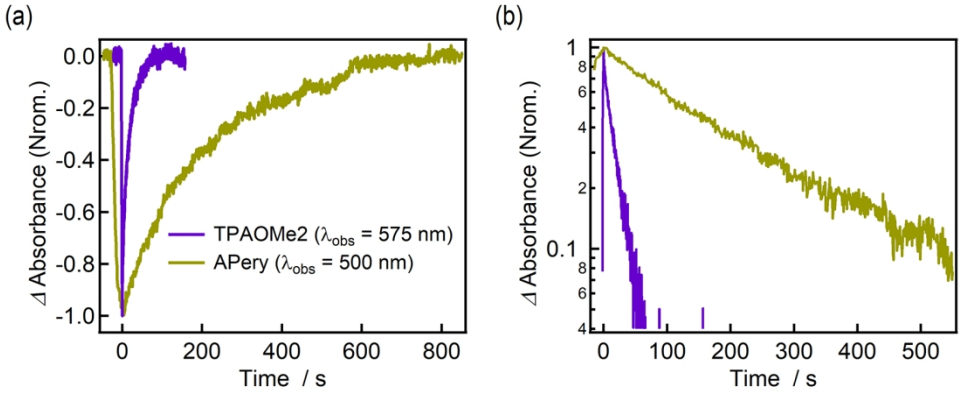

78x32mm (594 x 594 DPI)

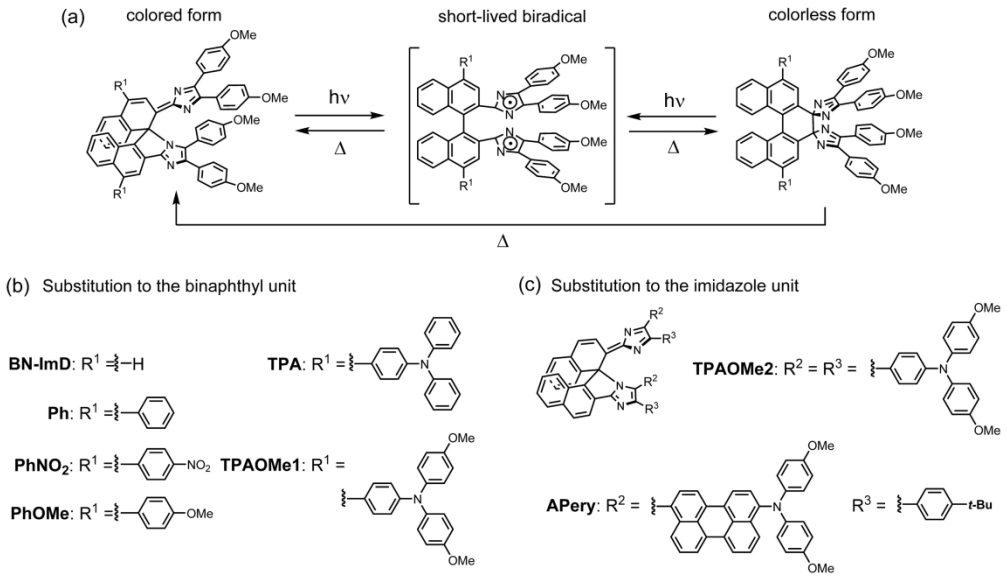

Scheme 1

123x70mm (600 x 600 DPI)

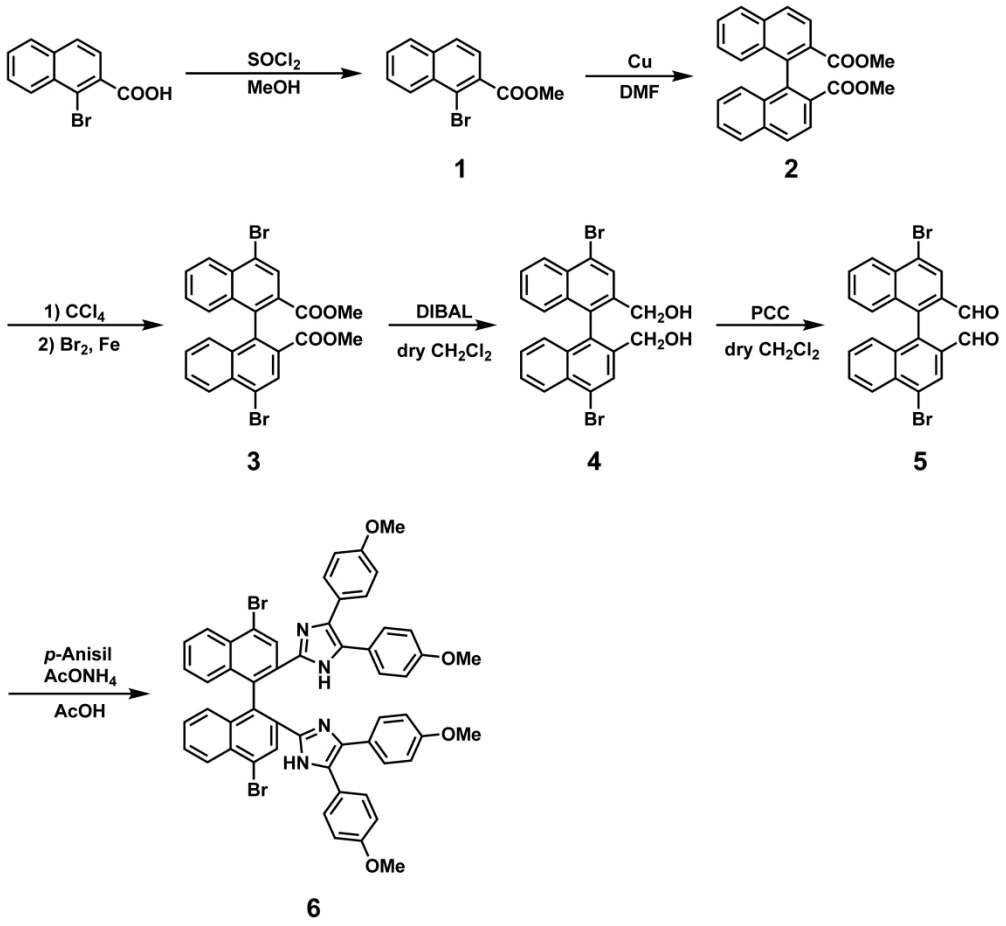
COOH
Br
SOCl2
MeOH
COOMe
Br
Cu
DMF
COOMe
COOMe
1
2
1) CCl4
2) Br2, Fe
Br
COOMe
COOMe
Br
DIBAL
dry CH2Cl2
Br
CH2OH
CH2OH
Br
PCC
dry CH2Cl2
Br
CHO
CHO
Br
3
4
5
p-Anisil
AcONH4
AcOH
OMe
Br
N
N
H
OMe
N
HN
OMe
Br
OMe
6

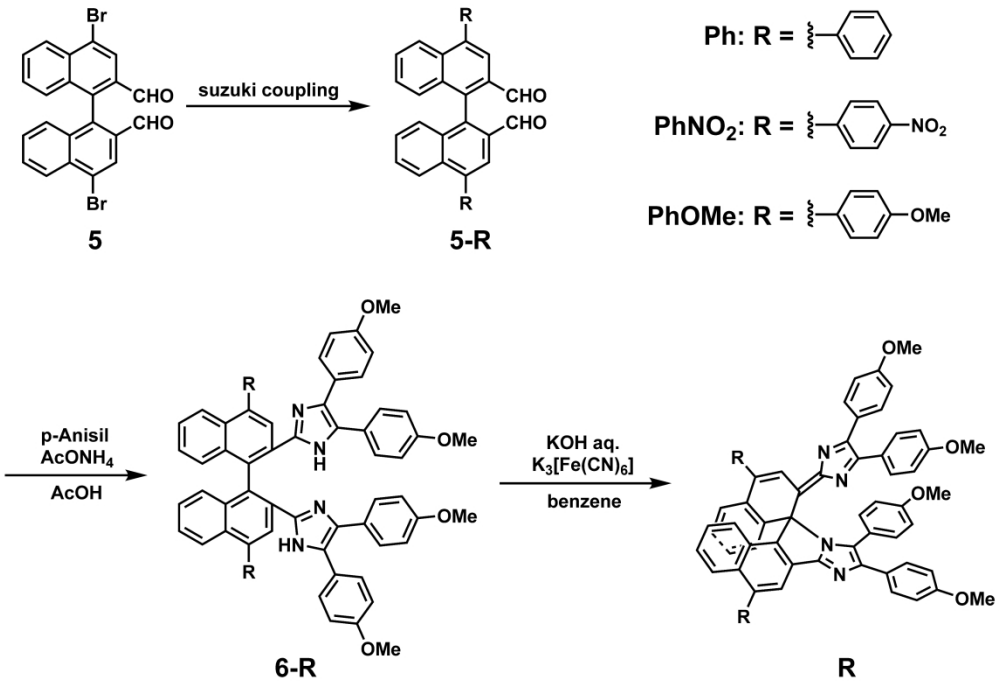
Br
CHO
CHO
Br
5
suzuki coupling
R
CHO
CHO
R
5-R
Ph: R =
PhNO2: R =
NO2
PhOMe: R =
OMe
p-Anisil
AcONH4
AcOH
OMe
R
N
H
N
OMe
HN
N
OMe
R
OMe
6-R
KOH aq.
K3[Fe(CN)6]
benzene
OMe
R
N
N
OMe
OMe
N
N
OMe
R
R

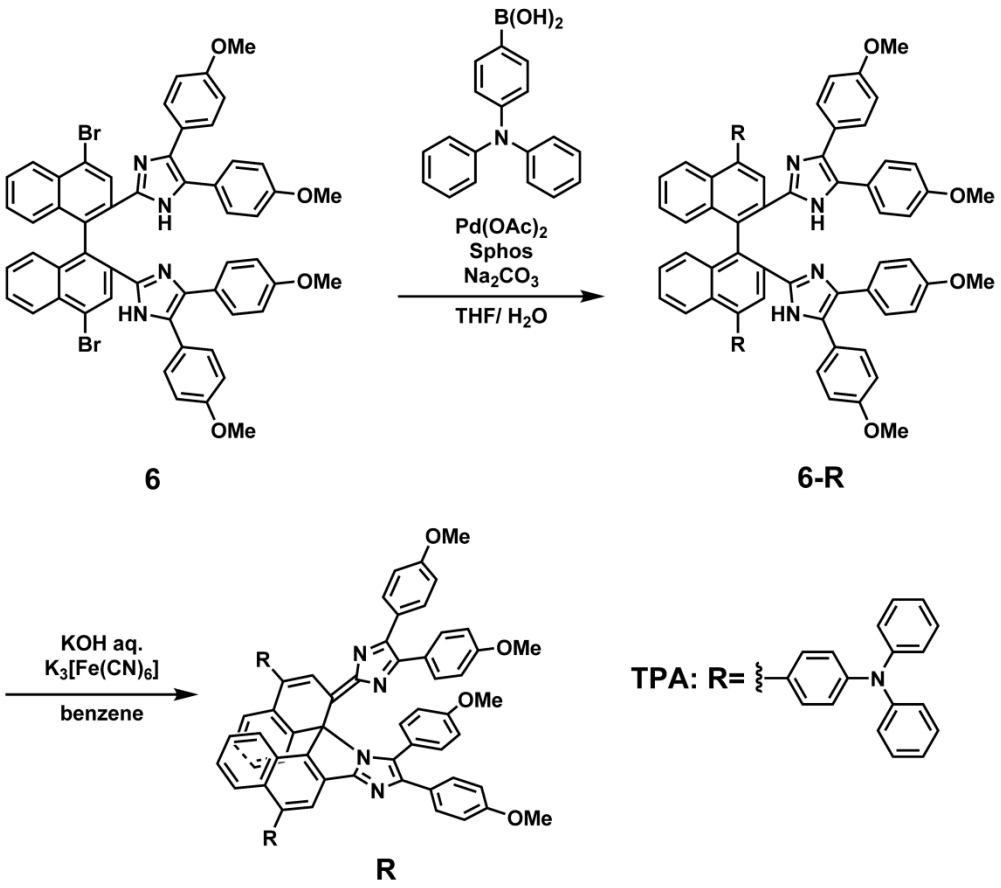
B(OH)2
OMe
Br
N
N
H
OMe
OMe
N
HN
Br
OMe
Pd(OAc)2
Sphos
Na2CO3
THF/ H2O
R
6
6-R
KOH aq.
K3[Fe(CN)6]
benzene
R
TPA: R=
N
R

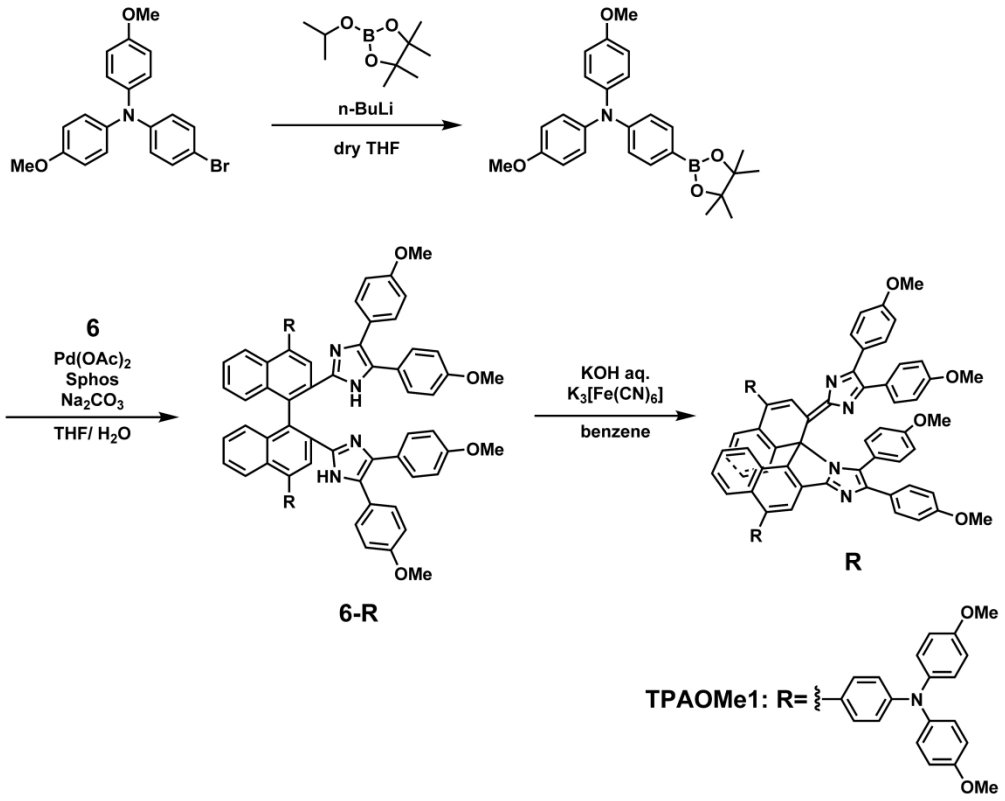
OMe
MeO
Br
n-BuLi
dry THF
6
Pd(OAc)2
Sphos
Na2CO3
THF/ H2O
6-R
KOH aq.
K3[Fe(CN)6]
benzene
R
TPAOMe1: R=

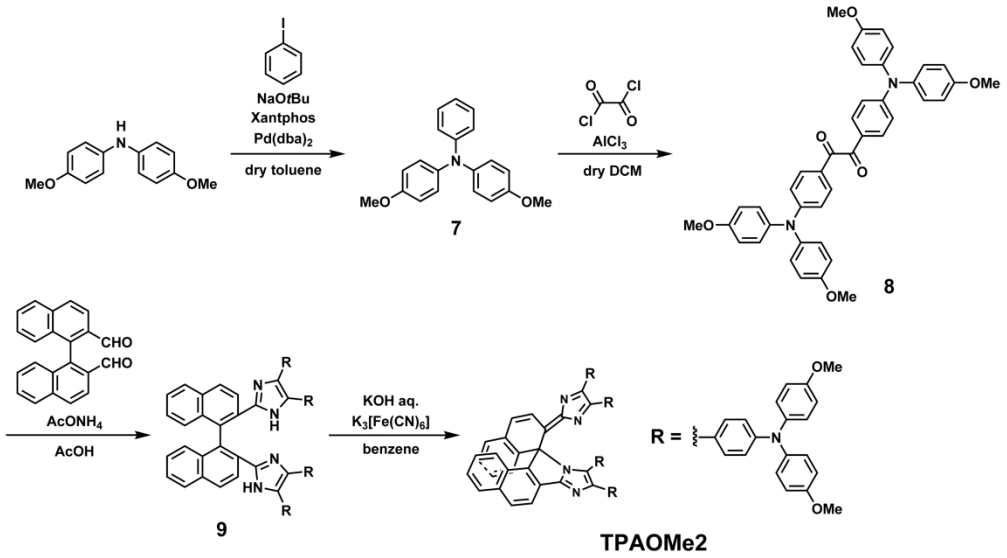
NaOtBu
Xantphos
Pd(dba)2
dry toluene
AlCl3
dry DCM
7
8
AcONH4
AcOH
KOH aq.
K3[Fe(CN)6]
benzene
9
R =
TPAOMe2

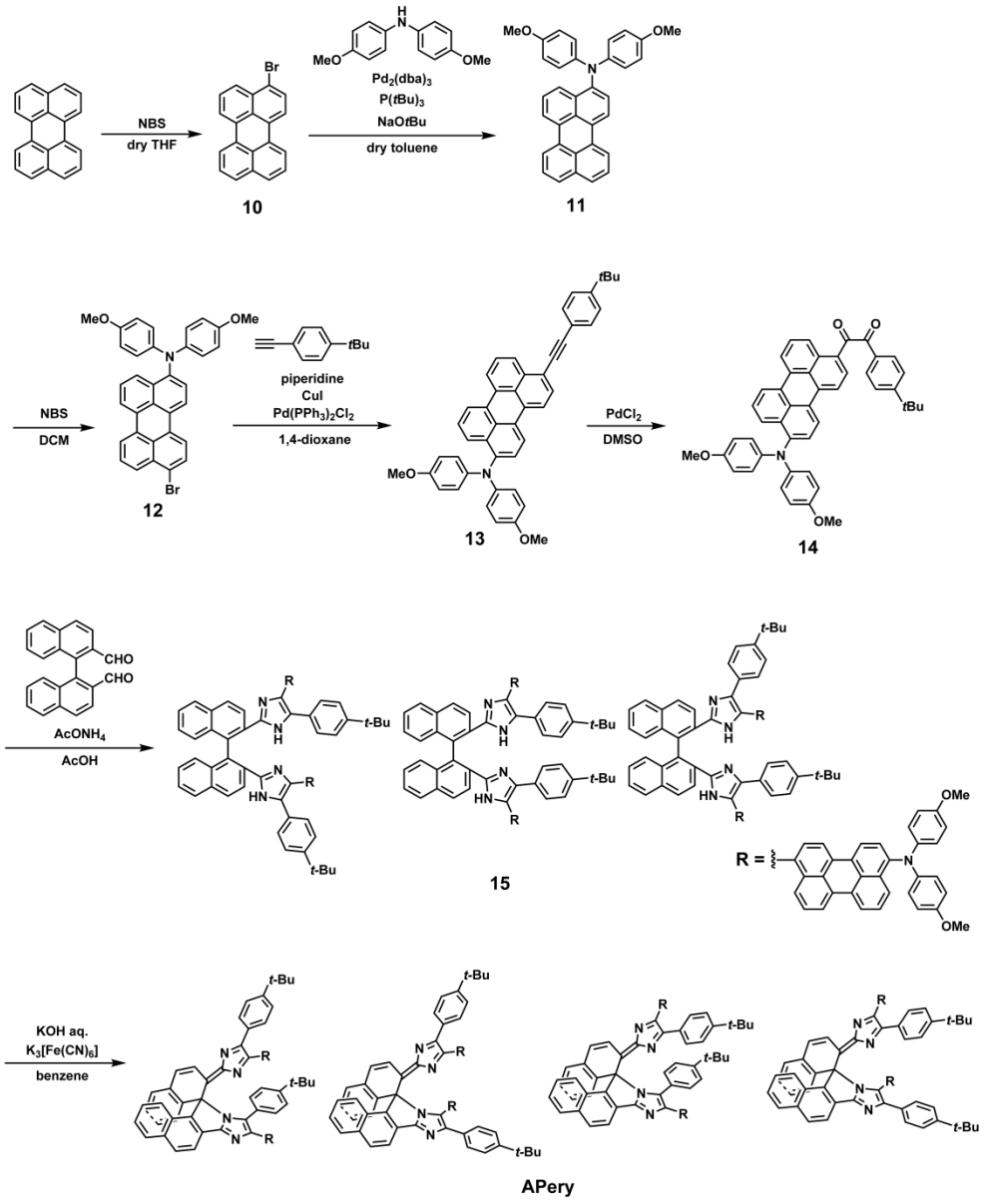
NBS
dry THF
Pd2(dba)3
P(tBu)3
NaOtBu
dry toluene
10
11
NBS
DCM
piperidine
CuI
Pd(PPh3)2Cl2
1,4-dioxane
PdCl2
DMSO
12
13
14
AcONH4
AcOH
15
R =
KOH aq.
K3[Fe(CN)6]
benzene
APery